Spring 2016

Effect of Quantum Dots, Novel Biological Imaging Agents, in Liver Cells in Vitro

Utshaha Maharjan
Central Washington University, maharjanu@cwu.edu

EFFECT OF QUANTUM DOTS, NOVEL BIOLOGICAL IMAGING AGENTS, IN LIVER CELLS *IN VITRO*

A Thesis

Presented to

The Graduate Faculty

Central Washington University

In Partial Fulfillment

of the Requirements for the Degree

Master of Science

Chemistry

by

Utshaha Maharjan

May 2016

CENTRAL WASHINGTON UNIVERSITY

Graduate Studies

We hereby approve the thesis of

Utshaha Maharjan

Candidate for the degree of Master of Science

APPROVED FOR THE GRADUATE FACULTY

_____ _____

Dr. Carin Thomas, Committee Chair

_____ _____

Dr. Levente Fabry-Asztalos

_____ _____

Dr. Todd Kroll

_____ _____

Dean of Graduate Studies

ABSTRACT

EFFECT OF QUANTUM DOTS, NOVEL BIOLOGICAL

IMAGING AGENTS, IN LIVER CELLS

IN VITRO

by

Utshaha Maharjan

May 2016

The use of Quantum dots (QDs) coated with polymer and functionalized with carboxylic acid groups in medical applications are explored. Their water solubility and exceptional stability in aqueous environments make them potentially useful for such applications as imaging and ligand attachments. However, there are concerns regarding the toxic effects of QDs and the minimal dose that can be used without producing any detrimental effects to organisms. In this study, QDs coated with the amphiphilic polymer coating tri-n-octylphosphine oxide and poly (maleic anhydride-alt-1-tetradecene (TOPO-PMAT)) which is functionalized with carboxylic acid groups were used to investigate their toxic effect in mouse liver cells. The cells were treated with 2 nM, 20 nM and 40 nM of QDs for a 24 -hour period and assays were performed to determine the effect on cell viability, ATP production, mitochondrial membrane potential and reactive oxygen

species (ROS) production. The results showed no significant effect on cell viability, ATP production and ROS production. However, the mitochondrial membrane potential of cells was significantly decreased when treated with 20 nM and 40 nM QDs. The results suggest that TOPO-PMAT QDs could be mildly toxic and precaution should be taken if used in higher concentration than 20 nM.

ACKNOWLEDGMENTS

I would like to thank my committee members, Dr. Carin Thomas, Dr. Levente Fabry-Asztalos and Dr. Todd Kroll for their support. Also, I would like to thank my family and friends for their help and encouragement.

TABLE OF CONTENTS

CHAPTER Page

TABLE OF CONTENTS (Continued)

CHAPTER Page

LIST OF FIGURES

TABLE OF CONTENTS (Continued)

Figure Page

CHAPTER I

INTRODUCTION

Nanoparticles and Their Uses

Nanoscience is the study and application of extremely small materials that can range from 1-100 nm in size.[1] The use of nanotechnology in medicine is spreading rapidly as a lot of biological events take place in nanoscale; for example, a strand of DNA is only about 2 nm in diameter, and hemoglobin, an oxygen carrying protein, is 5.5 nm in diameter. Engineered nanoparticles are explored for their possible use in drug delivery and cancer imaging and therapy. Due to their small size (1-100 nm) and relatively large functional surface area, these particles are able to bind, adsorb and carry other compounds such as drugs, antibodies and chemical fluorescence probes, and deliver them to targets in the body.[2] The main reason to use these nanoparticles in drug delivery is to decrease the side effects and toxicity of drugs used in the treatments.[2] Although these nanoparticles can be very useful for different purposes in medicine, there have been concerns that these nanoparticles could be toxic to the human biological system and may have detrimental effects on human body parts ranging from cell function to organ function such as lungs, brain and heart.[2]

Quantum Dots

There are several nanoparticles available such as nanotubes, nanowires, fullerenes and quantum dots (QDs). Among several nanoparticles, we are interested in QDs as they are fully described in terms of their chemical compositions and can be used for various medical applications.[3] QDs used in this study are highly stable in aqueous environments.[4]

Due to their high stability in aqueous environments they are very useful for biological imaging and the carboxyl functional group in the coating makes it convenient for ligand attachment for use in targeting specific cancers or cells.[5] There are various uses of QDs in photovoltaic cells, drug delivery, cancer imaging and as different biochemical probes. Similarly, further research has shown their promising use for *in vivo* applications by directing antibodies to cancer cell surface receptors and for siRNA delivery.[6]

The Chemical Composition of Quantum Dots

The chemical composition of QDs can be customized according to their uses. They usually consist of three parts: a core, a shell and a coating. There are several different types of cores, shells and coatings that can be customized according to the application. QDs have an inorganic semi-conductor core that determines their optical properties. The core of QDs are mostly composed of elements from groups III and V, such as InAs or GaN or groups IIB & VI, such as CdSe, CdS, CdTe, ZnSe, ZnS or ZnTe. The QDs whose cores are composed of elements from groups IIB and VI such as CdSe and CdS of periodic table emit visible light and are developed for biomedical purposes like diagnosis and cancer therapy. The shells in QDs are commonly composed of ZnSe, ZnS or CdS. Similarly, the QDs can be coated with various compounds depending upon their application, such as SiO_2, polymers and other molecules such as TOPO (tri-n-octylphosphine oxide). Also, they are often attached to biomolecules such as RNA, DNA, protein and lipids that are used to label cells or tissues, enter inside cells or deliver drugs to specific organs in the body. The physical properties of QDs such as solubility, charge, efficiency of optical emission and toxicity can be affected by its coating.[7]

In this study we are using TOPO-PMAT QDs provided by our collaborators at the University of Washington. The TOPO-PMAT QDs are made up of a CdSe core, a ZnS shell which are surrounded by a TOPO (tri-n-octylphosphine oxide), and a PMAT (poly (maleic anhydride-alt-1-tetradecene)) polymer coating (Figure 1). The intermolecular force that holds TOPO and PMAT are hydrophobic interactions. The hydrophobic interaction between TOPO and PMAT makes it very stable in aqueous solution which makes it very useful for medical purposes. The absorbance spectrum of these TOPO-PMAT QDs was determined to be between 400 nm to 500 nm and the fluorescence spectrum showed the maximum fluorescence emission at 620 nm (Figure 2).[8]

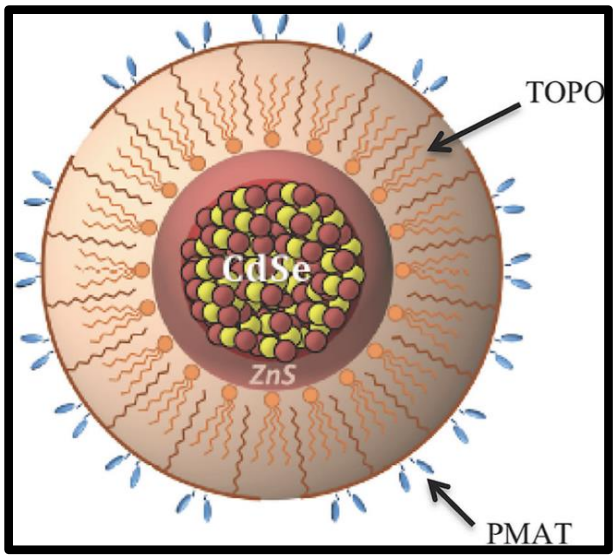

Figure 1: Diagram of TOPO-PMAT Quantum Dots.[8]

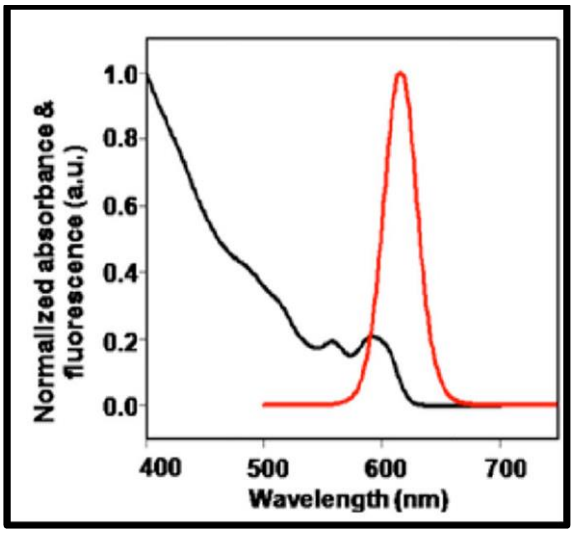

Figure 2: Maximum absorbance and emission of TOPO-PMAT Quantum Dots.[8]

Applications of Quantum Dots

TOPO-PMAT quantum dots are useful for biological imaging because of their high water solubility due to the carboxylic group attached to the outside and exceptional stability. These QDs can be used for molecular markers in cells instead of organic dyes and antibodies. Mortalin, a member of hsp 70 protein family which is a marker of transformed and normal cells depending upon its staining pattern can be stained easily with fluorescing quantum dots which otherwise requires several steps of staining with primary and secondary antibodies.[9] Kaul and colleagues showed that the mortalin staining pattern was uniform in cytoplasm and the perinuclear (space between the inner and outer layer of nucleus) in transformed (osteocarcinoma, U2OS) cells as reported previously by using the organic fluorescent dyes.[9] In addition, staining with QDs also provides longer fluorescence time. Mortalin stained with the organic dye “Alexa probe”

fades away after 3 minutes whereas the mortalin stained with QDs remained for 8 minutes giving longer and more accurate visualization.

Similarly, the presence of carboxyl functional groups in the coating of these QDs make them useful for ligand attachment. These kind of QDs can be modified accordingly for tumor targeting *in vivo* using antibodies directed to ligand surface receptors on cancer cells. Yang and colleagues coupled antibody (ScFvEGFR) with QDs to deliver the epidermal growth factor receptor (EGFR) in epidermal growth factor (EGF) expressing tumor *in vivo* mice models via tail vein. The result showed that there were large amounts of QDs bound to tumor cells in sections taken from frozen tumor tissues.[10] This shows that the QDs can be modified to target the tumor cells. Likewise, QDs can also be used for SiRNA delivery. SiRNA can be used in knocking down any type of mRNA which can be very useful in genomic studies and treatment of some tough diseases such as cancer. However, the delivery of siRNA *in vivo* is very difficult in practice which can be solved using QDs as a delivery vehicle. At least 50 copies of SiRNA were delivered to the targeted site by using TOPO-QDs in rats with xenograft prostrate tumors.[11] There are many probable applications of quantum dots in medical fields, and research is ongoing on the use of QDs in medical applications. However, there are concerns regarding the toxic effect of QDs when used for medical purposes.

Potential Toxic Effect of Quantum Dots

Despite their usefulness, concerns have been raised about QDs' potential toxic effects in organisms. There are several types of quantum dots depending on their uses.

They can be customized according to their uses and applications. They can differ in their structure, coating, size, diameter, surface charge, exposure time and the environment they are used in. These differences in manufacturing and use determine their stability which in turn determine the toxic effect of QDs in living organisms. Stable QDs are more resistant to photo-oxidation and remain intact for longer periods of time. Photo-oxidation is most likely to occur in unstable QDs and release the components of their cores, shells and coating resulting in cadmium related cytotoxicity to cells.[12] Unmodified “Naked" QD cores are known to produce reactive oxygen species which could be detrimental to organisms.[6] The induced reactive oxygen species could result in damage to biological membranes including plasma membranes and mitochondrial membranes.[7]

Due to multiple compositions and uses of QDs, their negative effect on biological systems is under intense study especially the toxicity of coating materials. Several QDs can be customized in terms of its shell and coating depending on their use, so it is very necessary to investigate the toxic effect on organisms. The proper surface coatings can reduce their toxic effect on organisms. Kim and colleagues investigated the effect of two differently coated QDs, one with 3 mercaptopropionic acid and another with tri-n-octylphosphine oxide (TOPO) in *Daphnia magna*. The experiment showed that the TOPO coated QDs caused a decrease in survival rate of *Daphnia magna* when treated with higher concentrations (100 µg/L) and 3 mercaptopropionic acid coated QDs treatment did not show any changes in survival rate across all the treatment concentrations.[12] One study showed that the CdSe QDs treated neuroblastoma cells

caused cell death via a cadmium-induced mitochondrial apoptosis pathway due to formation of reactive oxygen species. [13]

In another study, toxicity of QDs coated with polyethylene glycol (PEG) in different conditions were tested in zebrafish.[14] Zebrafish were treated with both oxidatively degraded and non-degraded PEG-coated QDs for 48 hours. The result showed that both degraded and non-degraded QDs had increased effect in death of zebrafish. However, the degraded QDs produced a severe effect when tested for morphological deformities such as pericardial, ocular and yolk sac edema. The weathered or oxidatively degraded QDs produced more pronounced morphological disorder even in lower concentrations (20 μM). The quantum dots coated with organic-COOH showed decreased cell viability at the lower concentration of 20 nM when treated up to 24 hours while the QDs coated with PEG showed reduced cell viability at 80 nM treated up to 48 hours in murine macrophages cells.[15] There are several studies for determining the cytotoxic effect of QDs on cells but the doses used varies from one study to another. Similarly, studies have shown that QDs with amphiphilic or protein coatings or ZnSe or ZnS shell are less cytotoxic.[16]

Similarly, the size of QDs affects their distribution and retention time *in vivo*. QDs' coating diameter determine the fate of their accumulation or excretion. QDs are excreted via urine if the hydrodynamic diameter is less than 5.5 nm. If the diameter is bigger than 5.5 nm, there is a chance that these QDs are deposited in liver.[17] Also, the same study determined that the increasing hydrodynamic diameter increases blood half-

life. Another study reported that the smaller sized QDs accumulated in liver within 1 hour of treatment and later accumulated in liver (15-80 days exposure) and the large QDs accumulated in spleen.[18] Similar studies done with PEG chains of different length which resulted in different hydrodynamic radii, showed that the increase in PEG length increased the retention time of QDs in liver.[19]

Surface charge of the QDs also plays an important role in determining the toxicity of QDs. Some research has shown that negatively charged QDs are less toxic than positively charged QDs. Some biological applications of QDs requires the use of positively charged QDs such as in the SiRNA delivery process.[11] Quantum dots with negatively charged coatings PEG-COOH or positively charge coating PEG-NH_2 caused severe coagulation and pulmonary thrombosis at the highest dose.[20] Another study done using similar (PEG-COOH and PEG- NH_2) QDs showed that the cytotoxic effect starts to appear when treated with doses of 20 nM after 24 hours of exposure.[21] A similar study showed that coating of QDs determines the subcellular localization of QDs. PEG-NH_2 coated QDs were localized in lysosomes and mitochondria while the non-functionalized PEG coated QDs were distributed evenly throughout the cells.[15]

In addition to the structures of coating, the stability of QDs also depend upon the environment of their use. Decreased growth rate was observed in Gram-positive *Bacillus subtilis* and Gram-negative *Escherichia coli* when treated with QDs dissolved in solutions weathered in different pH values. The toxic effect was due to the degradation and release of their coating, shell and core materials.[22] Kim et. al., (2010) exposed QDs

coated with TOPO and 3 mercaptopropionic acid to different forms of light such as white fluorescence light with or without UV-B for two days. The *Daphnia magna* exposed to TOPO-QDs exposed to UV-B for 2 days showed a significant rise in production of reactive oxygen species (ROS). In another experiment, the ability of QDs to withstand the intracellular conditions was determined by treating kidney epithelial cells with QDs. The result showed that the structure of QDs were not intact and leaked the cadmium out of its core. The acidic and oxidative environment of the lysosome could be responsible for the breakdown of QDs. Studies have shown that hypochlorous acid and hydrogen peroxide degrade the QDs' polymer coating, resulting in the release of core components.[22]

Toxicity can also be affected by the exposure time. *In vivo* studies have shown that the QDs can remain in mice up to two years and in some tissues up to 4 years inside a body of an organism. When these are accumulated *in vivo* these also show the blue shift in fluorescence. The blue shift is due to the loss of cadmium and selenium ions from QDs which imply that the QDs used are being degraded.[23]

Mechanism Behind Negative Effect

The mechanism of the negative effect of QDs on cells is not fully understood but the evidence has shown that cadmium binds and deactivates thiol (sulfhydryl) groups on iron-sulfur proteins that are essential for proper cellular and mitochondrial function.[24] One way to monitor the effects of QDs on living organisms is studying their effect on the subcellular organelle, the mitochondrion, as it is considered the powerhouse of cells due

to its capability of producing energy in the form of ATP which is required for proper functioning of cells.

Mitochondria

Most eukaryotic cells consist of these subcellular organelles, mitochondria that are approximately 10 μm in size. The number of mitochondria present in cells depends upon their metabolic capabilities. They consist of two membranes, outer and inner membranes, with an intermembrane space in between (Figure 3). The outer membrane is permeable and the inner membrane is highly selective compared to the outer membrane and only allows some substances to pass depending on the transport system. The inner membrane surface area is large due to numerous foldings called cristae. Inside the inner membrane is a compartment filled with different enzymes known as the matrix. The double membrane structure plays an important role in ATP synthesis and in apoptotic signaling pathways. In the inner membrane, the mitochondrial electron transport chain is located and ATP synthesis occurs by the process of oxidative phosphorylation. Mitochondria are also responsible for the metabolism of fats and proteins and the removal of toxic ammonia via the urea cycle and for signaling apoptosis or programmed cell death. The proper functioning of mitochondria is necessary for healthy and active cells and tissues. Studies have shown that mitochondrial dysfunction may be tied to various metabolic and degenerative diseases such as Parkinson's, atherosclerosis, cancer, cardiovascular disease, type II diabetes and dementia.[25]

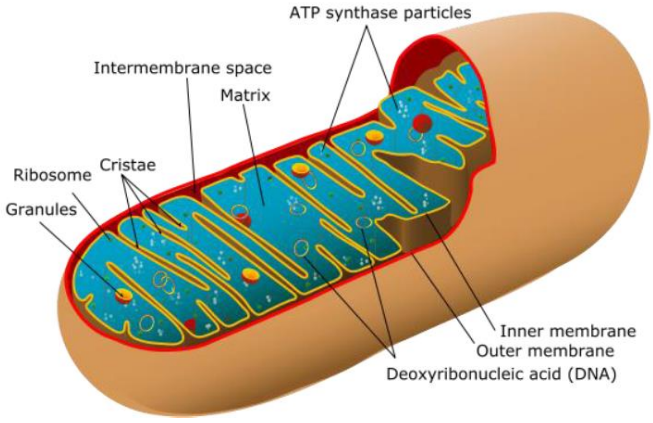

Figure 3: A mitochondrion showing inner membrane, outer membrane, intermembrane space, matrix and cristae. [26]

ATP Synthesis

The majority of ATP required for proper functioning of cells is produced by the process of oxidative phosphorylation which includes functions of the electron transport chain and F_0F_1 ATP synthase located in mitochondria. The inner membrane of mitochondria consists of four enzyme complexes which are coupled with the enzyme complex necessary for ATP synthesis, the F_0F_1 ATP synthase by a proton motive force. The four complexes, complex I (NADH: ubiquinone oxidoreductase), complex II (Succinate: ubiquinone oxidoreductase), complex III (Ubiquinone: cytochrome c oxidoreductase) and complex IV (cytochrome c oxidase) use several oxidation-reduction reactions to harvest electrons from the substrates nicotinamide adenine dinucleotide (NADH) and succinate. The harvested electrons are used to reduce the final electron acceptor molecular oxygen to water and create a proton gradient. Electrons flow from complex I and II (lower reduction potential) to complex III and IV (higher reduction

potential). The energy produced from oxidizing substrates is used in pumping protons across the inner membrane to the intermembrane space, which results in a proton gradient and an electrochemical potential across the inner mitochondrial membrane known as the mitochondrial membrane potential.[25] In the electron transport chain, the electron from complex I or II (NADH or succinate) is transferred to the oxidized form of coenzyme Q or ubiquinone resulting, in reduction of coenzyme Q. The reduced form of coenzyme Q is called ubquinol, which migrates towards complex III. During this process, complex I is able to pump protons towards the intermembrance space. At complex III, ubquinol is oxidized again, one electron at a time, and the electrons within the membrane are transferred to cytochrome c. From cytochrome c, the electrons are transported to complex IV. In complex IV, electrons are transferred to molecular oxygen, generating 2 moles of water per mole of oxygen. In addition, complex IV also drives protons across the membrane creating a proton gradient. The proton gradient is used by F_0F_1 ATP synthase to produce ATP from ADP and phosphate ions. During ATP synthesis, the created proton motive force activates the catalyst to drive the reaction between ADP and phosphate ions to produce ATP. In this way, active healthy mitochondria are able to use oxygen, form water, and maintain the ATP levels in cells through oxydative phosphorylation (Figure 4). However, during this process, reactive oxygen species are produced as a by-product of the reaction.

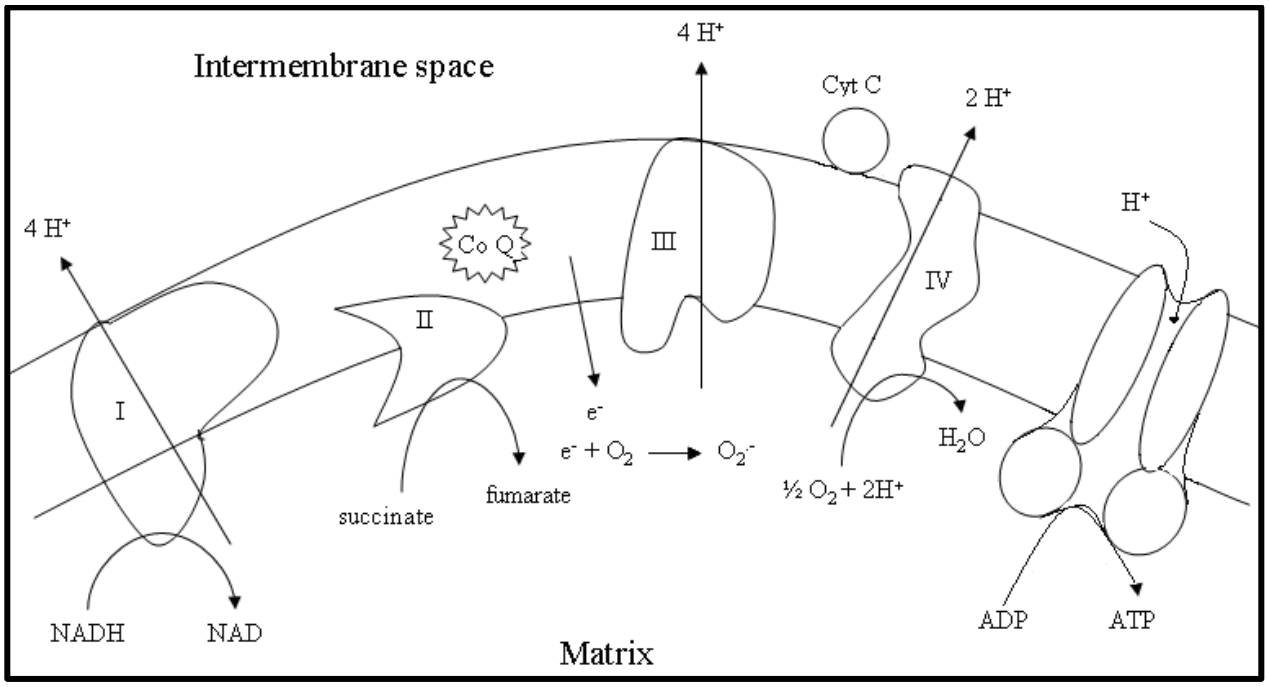

Figure 4: Electron transport chain and F_0F_1 ATPase showing oxidative phosphorylation and ROS production.[27]

ROS Production

The mitochondrial electron transport plays an important role in producing ATP which is very essential for life. However, during the process a small amount of electrons leak and react with oxygen which results in the formation of reactive oxygen species (ROS). The first ROS produced by mitochondria is superoxide anion radical. In the electron transport chain (ETC) oxygen is reduced to water through a four electron reduction on the surface of complex IV. However, some oxygen is converted to superoxide by a one-electron reaction with ubisemiquinone. This is converted into more stable hydrogen peroxide (H_2O_2) due to the action of Mn-superoxide dismutase (SOD) present in the matrix of mitochondria. The converted H_2O_2 can be removed by the

antioxidant system comprised of catalase and glutathione peroxidase. In addition, H_2O_2 produced in mitochondria also acts as a signaling molecule in the cytosol affecting multiple networks such as cell cycle and stress response. If there is an excessive amount of H_2O_2 production due to excessive stress on cells, the antioxidant system of cells may not work efficiently to remove it. As a result, H_2O_2 may generate hydroxyl radical ($OH^{\cdot}$), which is very reactive and is responsible for damaging any molecule it comes into contact with.[25] Hence the measure of H_2O_2 produced in cells can be used as a tool for measuring the oxidative stress caused by ROS.

Since mitochondria are very important organelles for the well-being of cells and are responsible for the generation of power for proper functioning of cells, studying the effects of QDs on this organelle is an effective way to monitor the toxicity of QDs in living organisms. The well-being of cells results in proper functioning of tissues and proper functioning of tissues results in proper functioning of organs, which in turn results in the well-being of an organism. Previous studies in the Thomas lab have shown that the mitochondrial functions are negatively affected after treating cells with QDs for 24 hours.[27] In this experiment, we are treating mouse liver cells with three different concentrations of QDs for 24 hours and monitoring their effects on the proper functioning of cells.

Liver Cells as Models for Quantum Dots Toxicity Studies

Biodistribution *in vivo* studies in Sprague-Dawley rats showed that QDs are initially targeted to liver and spleen.[28] The core metal of QDs, Cd was present in 0.92 µg Cd g^{-1} after 24 hours of injection and 1.69 µg Cd g^{-1} after 30 days of injection.[28] Since liver is the major target organ for QDs, liver cell culture models for the safety assessment of QDs would be relevant and applicable. The biological model used should be able to produce a reliable prediction when eventually used in *in vivo* systems. The measurement of toxicity in *in vitro* cultured liver cells would be comparable to the effect of quantum dots in liver. The liver is one organ which breaks down and metabolizes the toxins from all parts of the body and excretes them as harmless by-products into the bile, the intestine and feces. When using quantum dots for biological imaging or any other medical purposes, QDs will probably be routed to the liver. Thus the cytotoxicity assays done in mouse liver cells would be an excellent model to predict the effect of QDs in liver.

CHAPTER II

METHODS AND MATERIALS

In this experiment, Hepa-V cells lines were obtained and maintained in the laboratory. A total of four assays were conducted in this study. In the first two assays, cell viability assay and ATP luminescence assay, cells were plated in a 96 well plate, and in another two assays, mitochondrial membrane potential assay and reactive oxygen species (ROS) assay, cells were plated in a 24 well plate. The number of cells plated were 5000 cells/100 μL for 96 well plate assay and 10^5 cells/mL for 24 well plate assay. The details of the procedures are listed below.

Cell Culture and Passage

The Hepa-V hepatocyte cell line was obtained from collaborators at the University of Washington. The media for cell growth was prepared by adding 50 mL of Nu-serum and 10 mL of 100 U/mL streptomycin in 500 mL of Dulbecco's Modified Eagle Medium (DMEM)/F12 medium. The cells were grown in the prepared growth medium at 37 °C in a 95% air and 5% CO_2 humidified atmosphere in a 25 cm^2 tissue culture flask. The cell line was maintained by passing cells once or twice a week. For the passing of cells, the older media was removed and cells were washed with 3 mL of phosphate buffered saline (PBS) at pH 7.4. After washing, cells were treated with 1.5 mL of 0.05% trypsin dissolved in PBS for two minutes at 37°C in a 95% air and 5% CO_2 humidified atmosphere. The treatment of cells with trypsin detached cells from the bottom of the flask. After cells were detached from the bottom 5 mL of media was added

to stop the activity of trypsin. The mixture of media and trypsin was then transferred to a sterile conical tube and centrifuged at 800 rpm for 6 minutes. The trypsin and media mixture was aspirated and the pellet of cells in the bottom of a conical tube was re-suspended in 5 mL fresh media. 1 mL of resuspended cells in fresh media was taken and transferred to a sterile flask and 4 mL of fresh media was added. The new flask was incubated at 37 °C in a 95% air and 5% CO_2 humidified atmosphere. This process of transferring cells from one flask to the other is known as passage of cells. Cells from passage 1 through 9 were used in this study.[8, 29]

From the remaining resuspended cells in 5 mL of fresh media, 100 μL of the cell suspension was removed and diluted with 200 μL of water, then 10 μL of that solution was added to a hemocytometer and the number of viable cells was counted under the inverted microscope.

Counting Cells using a Hemocytometer and Plating Cells for Experiments

A hemocytometer microscope slide has etching or markings that consists of four large clear squares on the corners divided into 16 smaller squares each. The detail on the hemocytometer can be seen in figure 5. After 10 μL of diluted cell sample was applied to the hemocytometer, a coverslip was placed on the cells. Cells in each of those four squares including one large central square in the middle were counted. The average number of viable cells counted under an inverted microscope on these five large squares were calculated by dividing the total number of cells counted by 5. The total number of cells present in each mL of media was determined by using the following formula:

average number of cells counted in 5 squares of the hemocytometer X dilution factor X 10^4. After the number of cells per mL was determined, the cells were diluted using cell growth media to 5000 cells/ 100 μL for a 96 well plate assay and 10^5 cells/ mL for a 24 well plate assay.

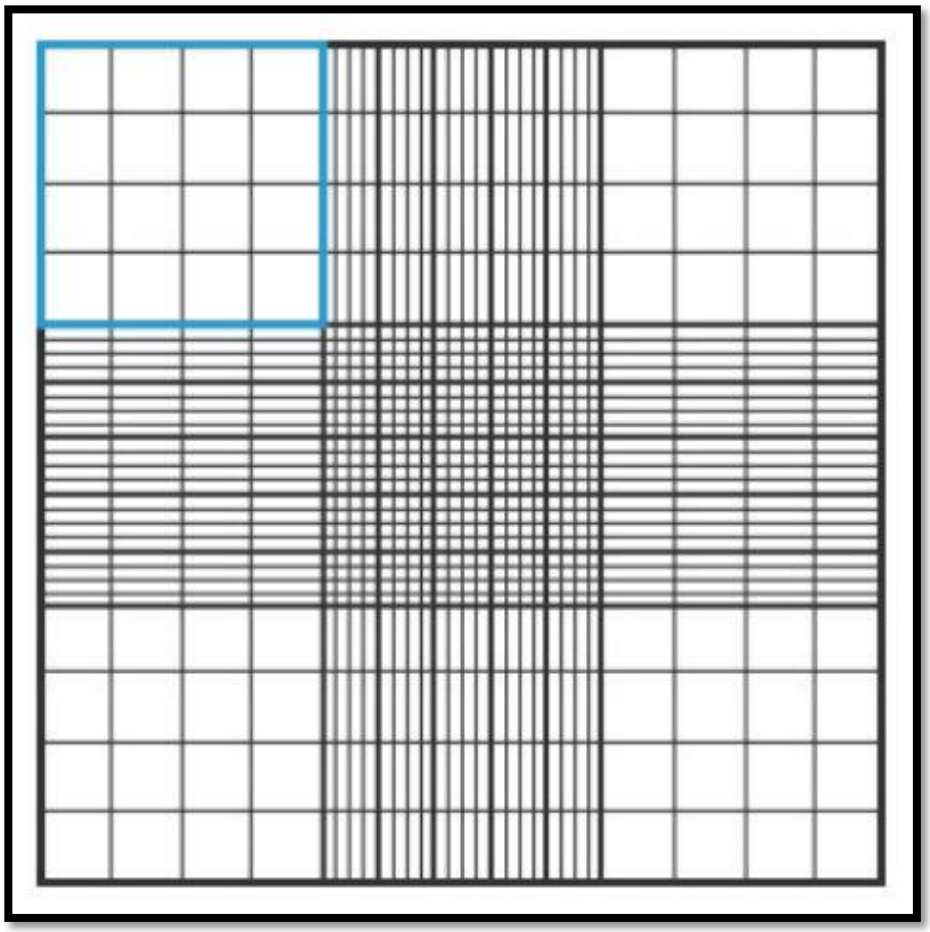

Figure 5: Glass hemocytometer diagram showing square spaces used in counting cells.

Treatment of Cells with Quantum Dots

TOPO-PMAT QDs were also provided by our collaborators at the University of Washington. QDs were stored in microfuge tubes wrapped in parafilm at room temperature inside a black conical tube to protect them from light. Cells were cultured in 96 or 24 well plates for 24 hours, and then treated with three different concentrations of QDs (2, 20 and 40 nM) for 24 hours at 37 °C and 5% carbon dioxide.[8] The stock solution of 900 nM of QDs in PBS was sterilized with a 0.22 μm filter attached to a sterile syringe. The sterilized QDs in PBS were diluted using an appropriate volume of DMEM medium with 10 % Nu-serum and 100 U/mL streptomycin. For 96 well plate assays, 100 μL of final volume was maintained and for 24 well plate assays the final volume of 400 μL was maintained for all three concentration of treatments. Following the 24-hour QDs treatment, the four assays were conducted.

Cell Viability Assay

The cell viability assay was used to determine the ability of cells to maintain or recover viability. It is an enzyme-based method that works by determining the mitochondrial dehydrogenase activity in the living cells. In this experiment we used a water-soluble tetrazolium salt, [2-(2-methoxy-4-nitrophenyl)-3-(4-nitrophenyl)-5-(2,4-disulfophenyl)-2H-tetrazolium, monosodium salt] (WST-8, Dojindo Inc.), which is a modified MTT (3-(4,5-dimethylthiazol-2-yl)-2,5-diphenyltetrazolium bromide) assay, to monitor the mitochondrial dehydrogenase activity of cells. WST-8 salts receive two electrons from viable cell mitochondrial dehydrogenases to generate an orange, yellow or

purple formazan crystal. The assay was used to monitor the effect of QDs on cell proliferation compared to untreated cells. In this assay, 5000 cells per 100 μL were plated and grown for two days or until cells were 80% confluent and treated with three different concentrations of QDs. On the day of assay, older media and QD treatment was aspirated and replaced with 90 μL of fresh media and 10 μL of WST-8 salt. One well was added with 90 μL of 40 nM QDs only and 10 μL of WST-8 salt which gave the background absorbance of QDs only. Then the cells were incubated for 4 hours at 37 °C and 5% carbon dioxide. After incubating for 4 hours, the contents of each well was transferred to unused wells and absorbance was read at 450 nm using a Synergy II plate reader. The background absorbance reading of QDs was subtracted from the absorbance value of QDs treated wells. The negative control used in this experiment was 20% dimethyl sulfoxide (DMSO). The working mechanism of WST-8 in determining cell viability can be seen in following reaction (Figure 6),

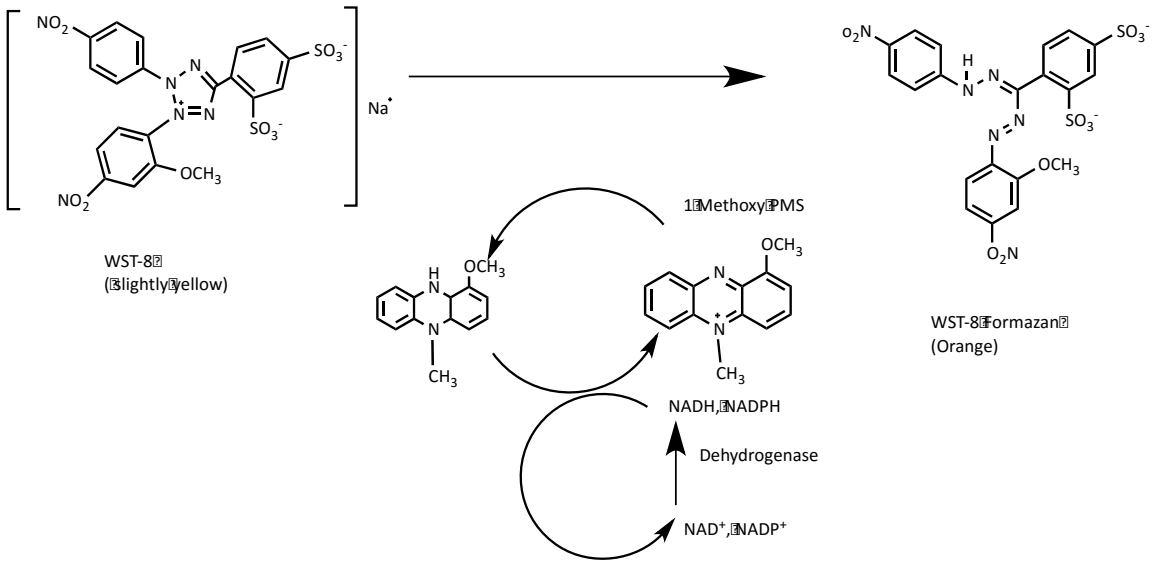

Figure 6: WST-8 reduction reaction in presence and absence of dehydrogenase. WST-8 is reduced by the dehydrogenase activity of cells into WST-8 formazan which is absorbed at 450 nm. Dehydrogenase is only produced by healthy cells and is proportional to the number of healthy cells. In absence or low amount of dehydrogenase, lower amount of WST-8 is converted to WST-8 formazan and absorbance at 450 nm decreases.

Adenosine Triphosphate (ATP) Luminescence Assay

Cells consume energy during their regular cellular processes of growth and metabolism. The required cellular energy form for these processes is adenosine triphosphate (ATP). When cells are treated with QDs, the amount of ATP produced by cells may be affected. The ATP luminescence assay was used to determine the amount of ATP in QD-treated cells compared to control cells. Cells were plated and treated similarly to the cell viability assay except a 96 well white luminescence plate was used. After the 24 hour QD treatment in 96 well plates, cells were washed with PBS buffer and treated with 35 μL of 1.5% triton X-100 at room temperature for 20 minutes. The

treatment of cells with Triton-X 100 solubilized the cell membranes to release cytoplasmic ATP. Then, 100 μL of assay solution (250 mM glycylglycin buffer, pH of 7.3, 2 mM EGTA, 2 mM $MgCl_2 \cdot 6H_2O$, 7.5 mM dithiothreitol, 15 μM luciferin and 10 μg/ mL luciferase) was added to the each well and the luminescence intensity of the reaction was measured immediately using a Synergy II luminescent plate reader with a plugged hole in the excitation filter wheel and a hole in the emission filter wheel. The ATP produced by cells in each well with the treatment of QDs was compared to the ATP produced by control cells and recorded as percent of control.[30] The amount of ATP produced in control cells was determined by the ATP standard curve with concentrations ranging from 10^{-6} to 10^{-9} nM by monitoring luminescence with a Synergy II plate reader. For positive control (lower amount of ATP production), cells were treated with 10 μM antimycin A for 6 hours and luminescence was quantified. 1 μL of 1 mM of Antimycin A stock solution prepared in 1:1 PBS and ethanol was taken and added to positive control wells resulting in final concentration 10 μM of antimycin A and 0.5% of ethanol in each positive control well. The reaction of ATP with luciferin in the presence of luciferase is shown in Figure 7.

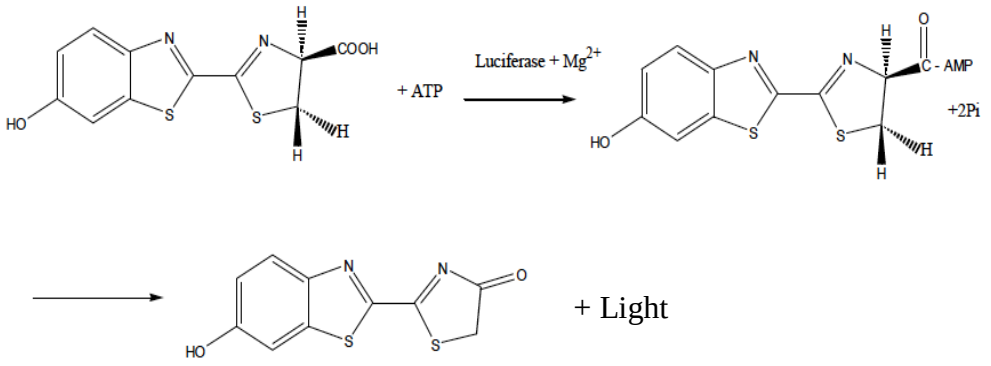

Figure 7: Reaction of luciferin and ATP in presence of luciferase.

Flow Cytometry

A flow cytometer (Bio-Rad S3e cell sorter) was used to collect data for two assays: the mitochondrial membrane potential assay and the reactive oxygen species (ROS) assay. Both of the assays used fluorescent dyes. The dye, JC- 10 was used for mitochondrial membrane potential assay. JC-10 dye exists as monomers in the cytoplasm and monomers aggregate to form J-aggregates inside the mitochondria in cells which was measured in two different excitation/ emission spectra in the flow cytometer. The filter 1 (FL1) channel measures the fluorochrome emission between 525 ± 30 nm and the filter 2 (FL2) channel measures fluorochrome emission between 586 ± 25 nm. In this case, the JC-10 dye is the fluorochrome. The JC-10 dye was examined for median fluorescence intensities using both of these channels and a fluorescence intensity ratio (FL2/FL1) was calculated. For the ROS assay only the median fluorescence intensity at FL1 was measured. Each experiment was performed until 50,000 events were collected. The

number of events refers to the number of single cells analyzed in the experiment. The collected number of events were analyzed by using a software program called FlowJo (V.10.1). FlowJo allows users to choose a population of cells to be analyzed, a process known as “Gating”. It is a process by which dead cells and debris that have been counted as events in the experiment are separated from the actual population of live cells being analyzed.

Mitochondrial Membrane Potential Assay

The mitochondrial membrane potential is related to the cell’s ability to make ATP. To monitor the effect of QDs on mitochondrial membrane potential, a lipophilic cationic dye JC-10 (Enzo Life Sciences) was used and analyzed using a flow cytometer in the Biology Department at CWU. Cells were plated in 24 well plates at 1 X 10^5 cells per mL and incubated until cells were 85 % confluent. After treating cells with QDs for 24 hours, QDs and media were aspirated and cells were washed with 200 µL of warm PBS. 6.7 µL of 1.5 mM JC-10 dye dissolved in 1:1 dimethyl sulfoxide (DMSO) and 20 mM 4-(2-hydroxyethyl)-1-piperazineethanesulfonic acid (HEPES) buffer in Hank’s Balanced Salt Solution (HBSS) with final pH of 7.3 with 0.02% pluronic F-127 and 493.3 µL of media was added to each well making the final concentration of dye to be 20 µM. The final concentration of DMSO in cells was maintained to be 0.67%. After the treatment of cells with JC-10, cells were incubated for 30 minutes at 37 °C in a 95% air and 5% CO_2 humidified atmosphere.[31] After the incubation, cells were washed with warm PBS and 200 µL of 0.05% trypsin was added. Cells were detached from the culture flasks and 500 µL of media was added to stop the activity of trypsin. Cells were transferred to a 5 mL

microfuge tube and centrifuged for 6 minutes at 800 rpm. Then the media and trypsin mix was aspirated and cells were re-suspended in HHBS buffer. Then the cell samples were analyzed using flow cytometry. QDs exposed cells treated with JC-10 produces green emission (JC-10 monomers) and orange emission (JC-10 aggregates) indicating low and high mitochondrial membrane potential, respectively. Fluorescence intensities from channels FL1 and FL2 were measured in cells by flow cytometry, the median fluorescence intensity was analyzed and determined using FlowJo. The ratio of fluorescence intensities at FL2/FL1 was calculated. For a positive control, cells were treated with 5 μM of carbonyl cyanide-4-(trifluoromethoxy) phenylhydrazone (FCCP) in ethanol for 10 minutes and then treated with JC-10 dye.[32] The 5 μM of FCCP was prepared from the stock solution of 1 mM FCCP dissolved in ethanol. 5 mL of the stock solution was added to 495 μL of media resulting in final concentration of 5 μM FCCP and 1.1% of ethanol.

Growing Cells for Fluorescence Microscopy

For the fluorescence microscopy experiment Hepa-V cells were grown on a cover slip. The 22 mm square coverslip was sterilized by spraying with 70 % ethanol and then with flame. The coverslip was placed in a 60 X 15 mm petri dish. 1 mL of cells resuspendend in 4 mL of DMEM/F12 was added to the petri dish. The cells were allowed to grow for 48 hours in 37 °C in a 95% air and 5% CO_2 humidified atmosphere. After 48 hours, media from the petri dish was removed and added with 3.0 mM JC-10 dye dissolved in 1:1 DMSO and 20 mM 4-(2-hydroxyethyl)-1-piperazineethanesulfonic acid

(HEPES) buffer in Hank's Balanced Salt Solution (HBSS) with final pH of 7.3 with 0.02% pluronic F-127 and DMEM/F12. Then the petri dish was incubated for 1 hour. Then, the petri dish contents were aspirated and the coverslip was washed with 5 mL of PBS twice. After washing, the coverslip was taken out of the petri dish using tweezers and placed inverted on a microscope glass slide. The coverslip was placed on the glass slide in such a way that the side on which cells were growing faced the glass slide. Two drops of PBS were added to the glass slide before placing the coverslip. Excess PBS after placing the coverslip was removed using a Kim wipe. After placing the coverslip in the desired position, it was sealed using clear nail polish on all 4 sides of the coverslip. After the nail polish dried, the whole slide was cleaned with lens cleaner and read under a fluorescence microscope and images were taken.[33]

Intracellular ROS Assay

The intracellular reactive oxygen species (ROS) production was measured using a fluorescent dye called CellRox green (Invitrogen, Inc.) and flow cytometry. Cells were plated at 100,000 cells / mL in 24 well plate and incubated until 85% confluent then cells were treated with QDs for 24 hours. On the day of the assay, the plated cells were aspirated and 498 μL of fresh media was added. 2 μL of 250 μM of CellRox green dye was then added to the cell plated wells and incubated for 45 minutes protected from the light giving a final concentration of CellRox green of 1 μM. After the incubation, the media was removed and cells were removed from the plate with trypsin and resuspended in FACS (fluorescence activated cell sorting) buffer which consists of 1% BSA and 0.1%

sodium azide buffer. For a positive control, 498 µL of 300 µM *tert*-butyl hydroperoxide (TBHP) diluted in media was added to the cells and incubated for 45 minutes.[34] TBHP reacts with ferrous iron to produce hydroxyl radical via a process of Fenton chemistry where the iron is oxidized by the TBHP (Figure 8).

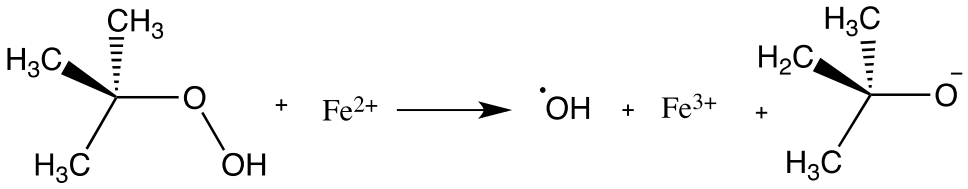

Figure 8: TBHP reaction with ferrous ion to produce hydroxyl radical, •OH.

Statistics

For each experiment, the data collected was averaged and standard deviation (Cell viability and ATP assay) or range (Mitochondrial membrane potential and ROS assay) were calculated. Data collected for each experiment was analyzed for statistical significance by using one-way ANOVA and the significance was set to $P \leq 0.05$. All the statistical analyses were done by using Microsoft Excel version 2013. The replicates for the experiments were 3 to 6.

CHAPTER III

RESULTS

Cell Viability

A cell viability assay was used to determine the effect of QDs on cell proliferation and the cytotoxic effects to cells that would eventually lead to cell death. Cell viability was evaluated by using a modified water soluble MTT assay. In this method, water soluble tetrazolium salt is reduced due to the activity of mitochondrial dehydrogenases. The measurement of activity of mitochondrial dehydrogenase produced by the active and healthy cells helps to determine the cell viability. Hepa-V cells showed a trend of decreased mitochondrial dehydrogenase activity when treated with 2 nM, 20 nM and 40 nM QDs. The trend showed that the cells treated with 2 nM, 20 nM and 40 nM QDs appear to have 21.5%, 20.9% and 13.8% decreased cell viability respectively (Figure 9). However, the decrease in dehydrogenase activity was not statistically significant ($P>0.05$) compared to control cells analyzed by one-way ANOVA. The positive control used in this experiment (20% DMSO) showed 73% decrease in cell viability. DMSO at concentrations higher than 10% causes cells to undergo apoptosis.[35]

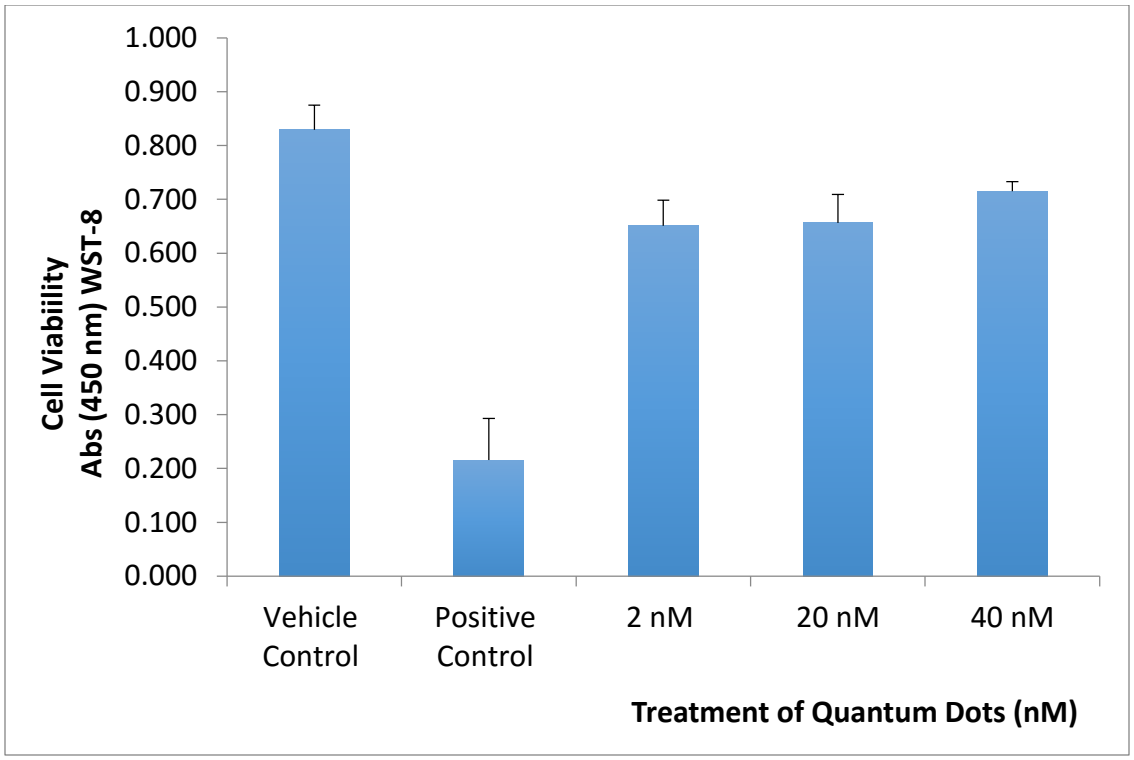

Figure 9: Cell viability in liver cells after 24-hr exposure to QDs. Liver cell mitochondrial dehydrogenase activity measured by the water soluble MTT assay (WST-8). Analysis by one-way ANOVA (p=0.08, n=6), indicates no significant effect of QDs on metabolic cell death. Positive control cells were treated with 20 % DMSO for 1 hr.

ATP Content in Cells

Adenosine 5'- triphosphate (ATP) is very crucial in biological systems for exchanging energy. It is produced and present in all metabolically active cells as an immediate free energy donor. The production of ATP in cells denotes the cellular integrity as cells require ATP for proper functioning. An ATP luminescence assay was used to determine the quantity of ATP produced by Hepa-V cells. In this method, the substrate luciferin was used which reacts with ATP in the presence of the enzyme

luciferase to produce light. The result showed that there was no significant decrease in ATP produced by cells when treated with different concentrations of QDs ($p>0.05$, one-way ANOVA). There was a trend of 2%, 2% and 14% decrease in ATP production by cells when treated with 2 nM, 20 nM and 40 nM QDs, respectively (Figure 10). However, it was not statistically significant.

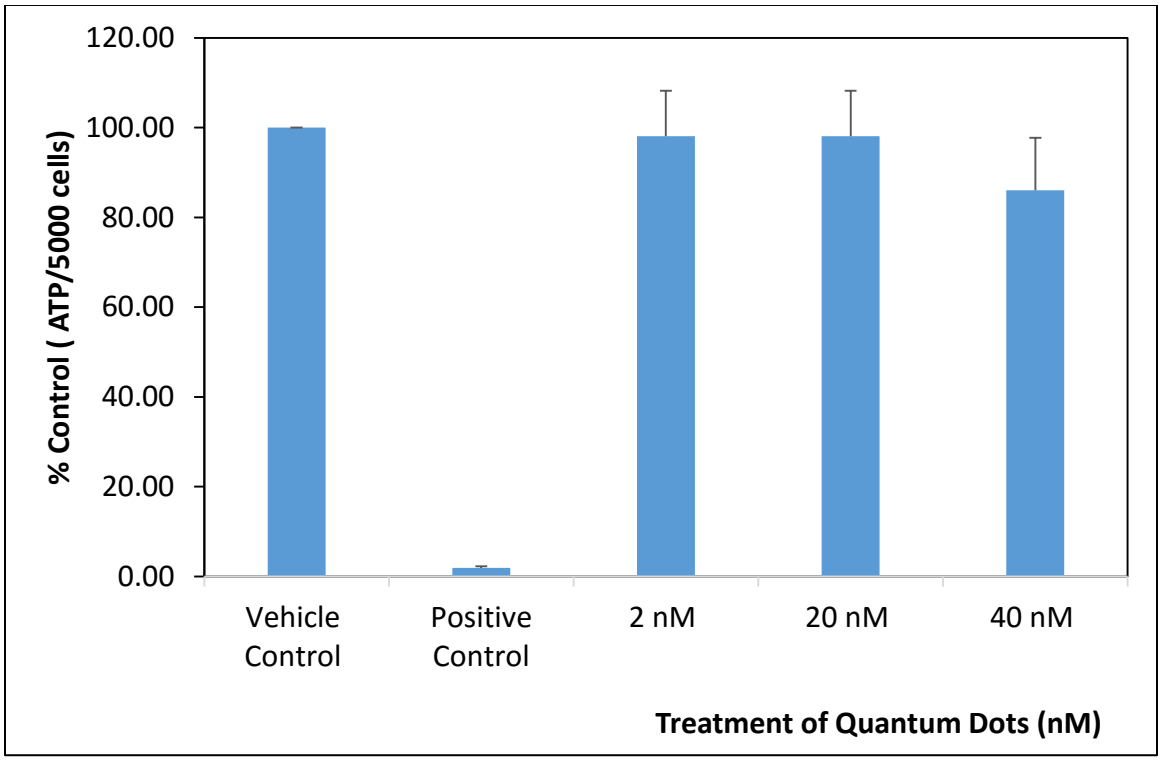

Figure 10: ATP production in liver cells after 24-hr exposure to QDs. ATP production of liver cells was determined by the Luciferase/luciferin luminescence assay. Control consists 1.5% Triton-X 100. Positive control cells were treated with 10 µM Antimycin A for 6 hours. Analysis by one-way ANOVA ($P= 0.17$, $n=6$) indicates no significant effect of QDs on ATP production of cells. ATP values of the control cells ranged between 42 nM and 88 nM per 5000 cells.

The positive control used in this experiment was 10 µM antimycin A which showed 98% decrease in ATP production. Antimycin A is an antibiotic which interferes

with electron flow from complex III to cytochrome C. In the presence of antimycin A cytochrome c remains oxidized, eventually stopping the process of ATP production.

Mitochondrial Membrane Potential Assay using JC-10

Mitochondria are considered to be the power house of cells since they generate ATP. The change in mitochondrial membrane potential ($\Delta\psi_m$) indicates the capacity of mitochondria to generate ATP and maintain cell health. In this experiment, a cationic lipophilic dye (JC-10) was used in order to determine $\Delta\psi_m$ in cells. JC-10 is a mitochondrial membrane permeable dye which can exist in its monomeric and J-aggregate forms depending on the $\Delta\psi_m$. As mitochondria become more polarized (increase $\Delta\psi_m$), more JC-10 enters mitochondria and JC-10 starts forming J- aggregates shifting the fluorescence emission from 530 nm to 590 nm, fluorescing red. In healthy cells, the amount of J- aggregate is always equal to or higher than that of the monomer. The result from fluorescence microscopy showed that the JC-10 dye used for the mitochondrial membrane potential assay appears to fluoresce both green (FL1) and red (FL2) uniformly in the cytoplasm of healthy cells (Figure 11).

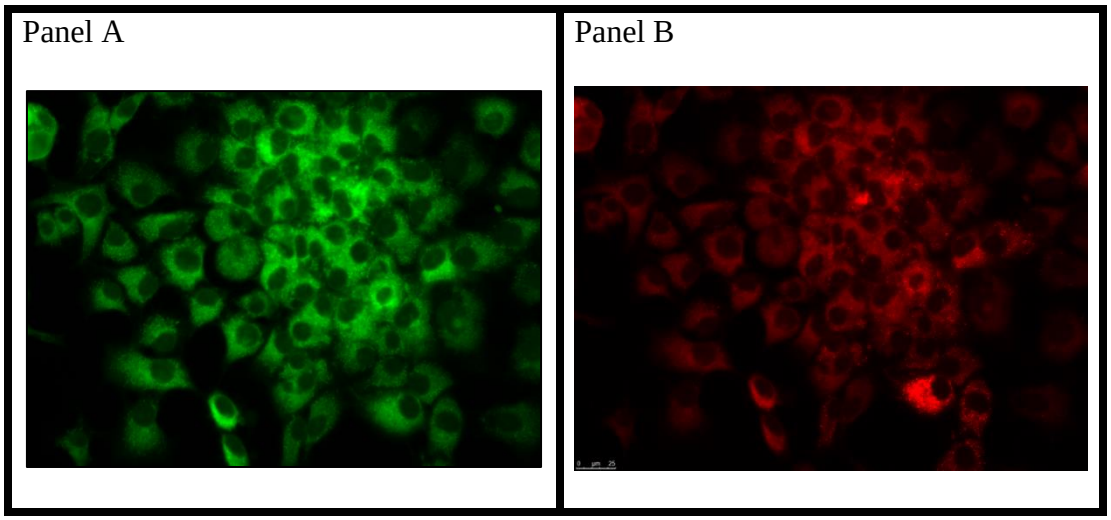

Figure 11: Fluorescence microscopy images of localization of JC-10 dye in Hepa-V cells. Cells were grown on a coverslip for 48 hours and treated with JC-10 dye for 45 minutes. Separate images were taken using different fluorescence filters for cells (panel A: ex/em: 488/530 nm and Panel B: ex/em: 488/590 nm)

As the mitochondrial membrane potential decreases, the amount of fluorescence at FL2 decreases and hence the ratio of FL2/ FL1.

A $\Delta\psi_m$ assay was performed using JC-10 dye and cells were analyzed using flow cytometry. The JC-10 dye forms J- aggregates which fluoresces with emission at 590 nm (FL2). In healthy cells with a high mitochondrial membrane potential, the accumulation of J- aggregates is equal to or higher than its monomeric form. The results showed that the ratio of FL2/ FL1 decreased as the concentration of QDs increased. The ratio of FL2/ FL1 is similar when compared between the control cells and cells treated with 2 nM QDs. The fluorescence intensity FL2/ FL1 ratio of cells treated with 20 nM and 40 nM significantly decreased compared to control cells ($P < 0.05$, one-way ANOVA) (Figure 12).

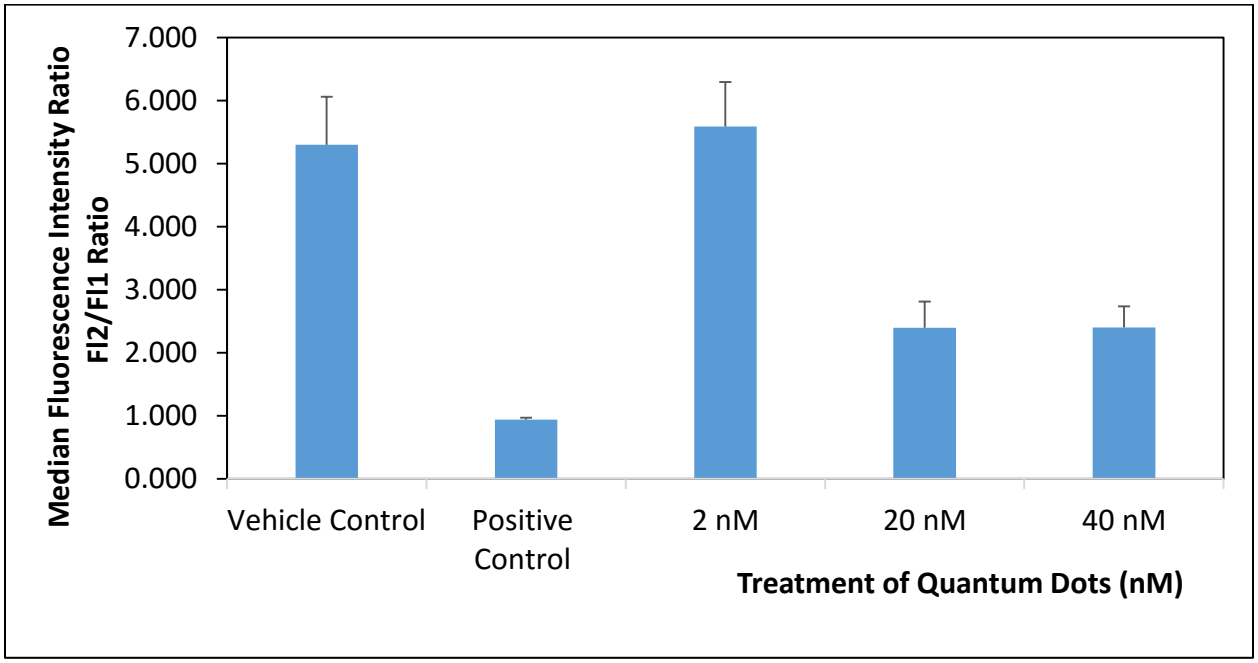

Figure 12: Mitochondrial membrane potential in liver cells after 24-hr exposure to QDs**.** JC-10 dye (20 µM) was added to Hepa-V liver cells and incubated for 30 min. Postive control cells were treated with FCCP (5 µM) and incubated for 10 min. The median fluorescence intensities for both J-aggregates and monomeric forms of JC-10 were measured, at Ex/Em = 488/590 nm and 488/525 nm with flow cytometry and their ratio was calculated (FL2/FL1). Analysis by one-Way ANOVA (P= 0.00017, n=2) indicates significant effect of QDs on $\Delta\psi_m$. Two values were averaged and the error bar represents the range of those values.

The decrease in FL2/ FL1 ratio showed that the amount of J- aggregates accumulated in mitochondria of cells decreased as the concentration of QDs increased in the cells. The decrease in amount of J- aggregates suggested that the mitochondrial membrane potential of cells was decreasing with increased concentration of QDs in cells. The positive control (FCCP) showed a decrease in mitochondrial membrane potential

denoted by decreased FL2/ FL1 ratio. FCCP uncouples the mitochondria as a result of which mitochondrial membrane potential decreases.[32]

Reactive Oxygen Species (ROS) Production in Cells

Cells produce reactive oxygen species (ROS) during the process of formation of ATP through oxidative phosphorylation. In normal conditions, cells have their own antioxidant mechanism to remove ROS. However, under stress cells may be making more ROS than they remove. The presence of ROS in cells is an indicator of stress due to exposure to chemicals such as QDs. In this experiment the ROS produced by cells when treated with QDs were measured by the fluorescence intensity of CellRox green dye which fluoresces brightly in the presence of reactive oxygen species and is detected using the FL1 filter in the flow cytometer. Due to limited amount of QDs, the experiment was performed two times only. The data for these experiments is questionable because the flow cytometer was clogged on the day of the experiment and cells were stored in refrigerator for more than two hours before analyzing in flow cytometer. We were unable to combine these two experiments together and do a statistical analysis on it.

The first experiment (trial 1) showed the decreased trend in production of ROS when treated with QDs compared to control cells. It showed that the production of ROS in cells treated with 20 nM and 40 nM had a decreased trend as compared to control cells but increased trend as compared to cells treated with 2 nM QDs. However, the positive control in the experiment also showed a decrease in ROS production. For the positive control, cells were treated with tertiary butyl hydrogen peroxide (TBHP), a known ROS producer with an expected result of increasing ROS (Figure 13, Panel A).

The second experiment (trial 2) showed similar trends. The production of ROS showed a decreased trend in cells treated with QDs as compared to control cells. The production of ROS in cells treated with 20 nM appeared to decrease as compared to control cells but appeared to increase as compared to the cells treated with 2 nM and 40 nM QDs. The positive control also showed an increase in ROS production which was expected (Figure 13, Panel B).

Even though the positive control did not work on the first experiment, the results are comparable in both the experiments. The trend of decreased ROS when treated with 2 nM QDs was similar in both experiments. When treated with 20 nM, QDs production ROS decreased as compared to control but increased as compared to 2 nM treatment and the trend is similar in both experiments. When treated with 40 nM QDs, the ROS production decreased as compared to control in both experiments. However, the ROS production with 40 nM QDs treatment was equal to ROS production when treated with 20 nM QDs in first experiment, whereas it decreased slightly in second experiment.

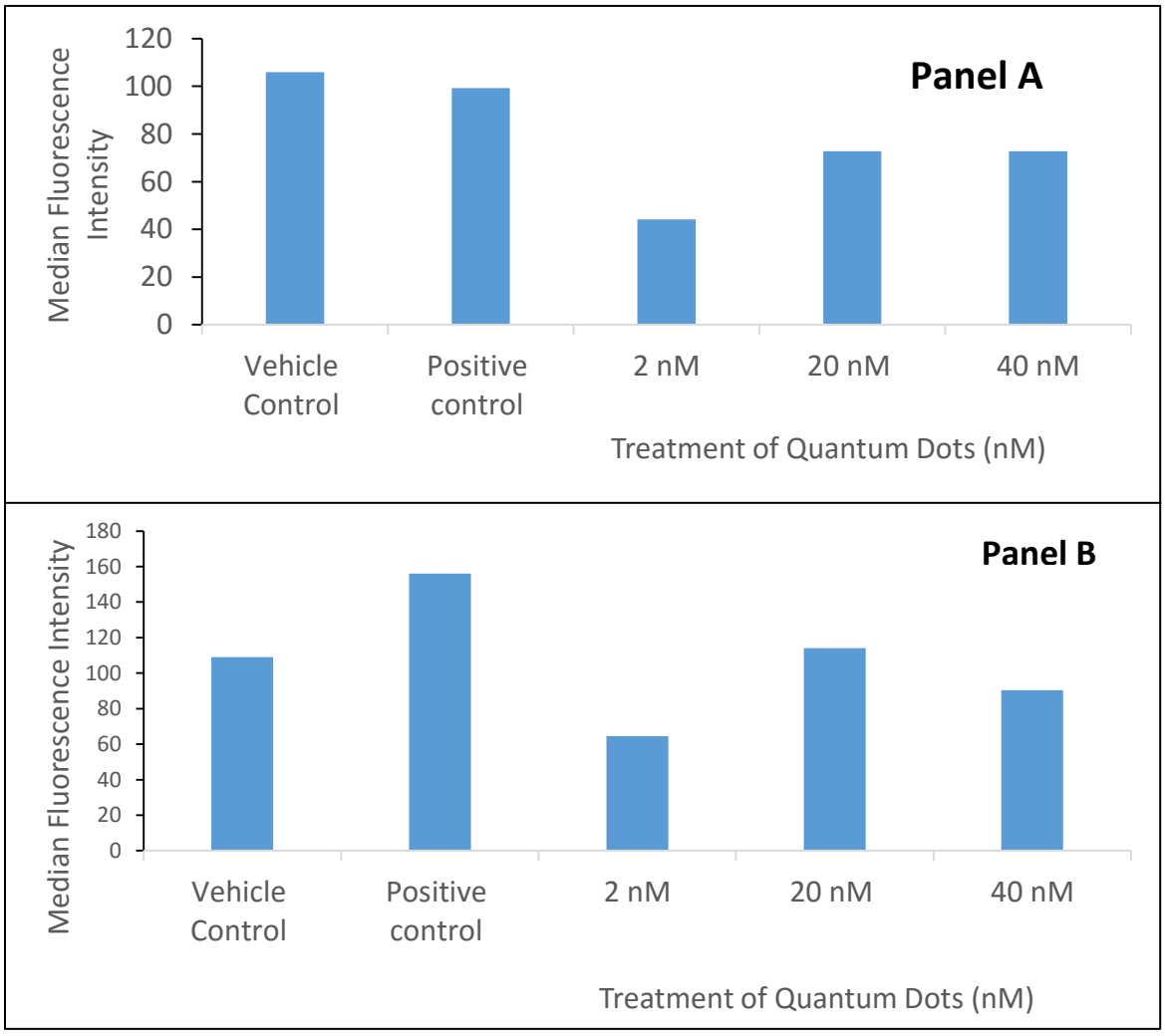

Figure 13: Production of reactive oxygen species (ROS) in liver cells after 24-hr exposure to QDs**.** CellRox green dye (1 µM) was added to Hepa-V liver cells and incubated for 45 min. Positive control cells were treated with 300 µM tertiary butyl hydrogen peroxide (TBHP) and incubated for 45 min. The median fluorescence intensities for CellRox green dye was measured at Ex/Em = 488/530 nm with flow cytometry (FL1 median fluorescence intensity). Panel A contains the data from Trial 1 and panel B contains the data from the Trial 2 of the experiment performed on the same day.

Comparison of Fluorescence of QDs and JC-10 Dye

The quantum dots used in these experiments have a maximum fluorescence emission at 620 nm which is measured with the FL3 filter on the flow cytometer.[8] However, the emission spectrum of QDs showed some overlap in emission at wavelength 590 ± 25 nm, which can be measured by using FL2 in the flow cytometer. The dye used in these experiments fluoresced and were analyzed and detected through FL1 or FL2 in flow cytometer. To show that the median fluorescence intensity of dyes used such as JC-10 and fluorescence of QDs did not overlap with each other, Hepa-V cells were treated with 20 nM of QDs and analyzed with flow cytometry using filters FL2 and FL3. The median intensity recorded for QDs at FL2 was 277 and at FL3 was 10,337 (Figure 14, Panel A left and right). We compared these median fluorescence intensities to the median fluorescence intensities of the cells treated only with JC- 10 dye. The fluorescence intensity for cells treated only with JC- 10 was 265 at FL2 (Figure 14, Panel B, and Left).

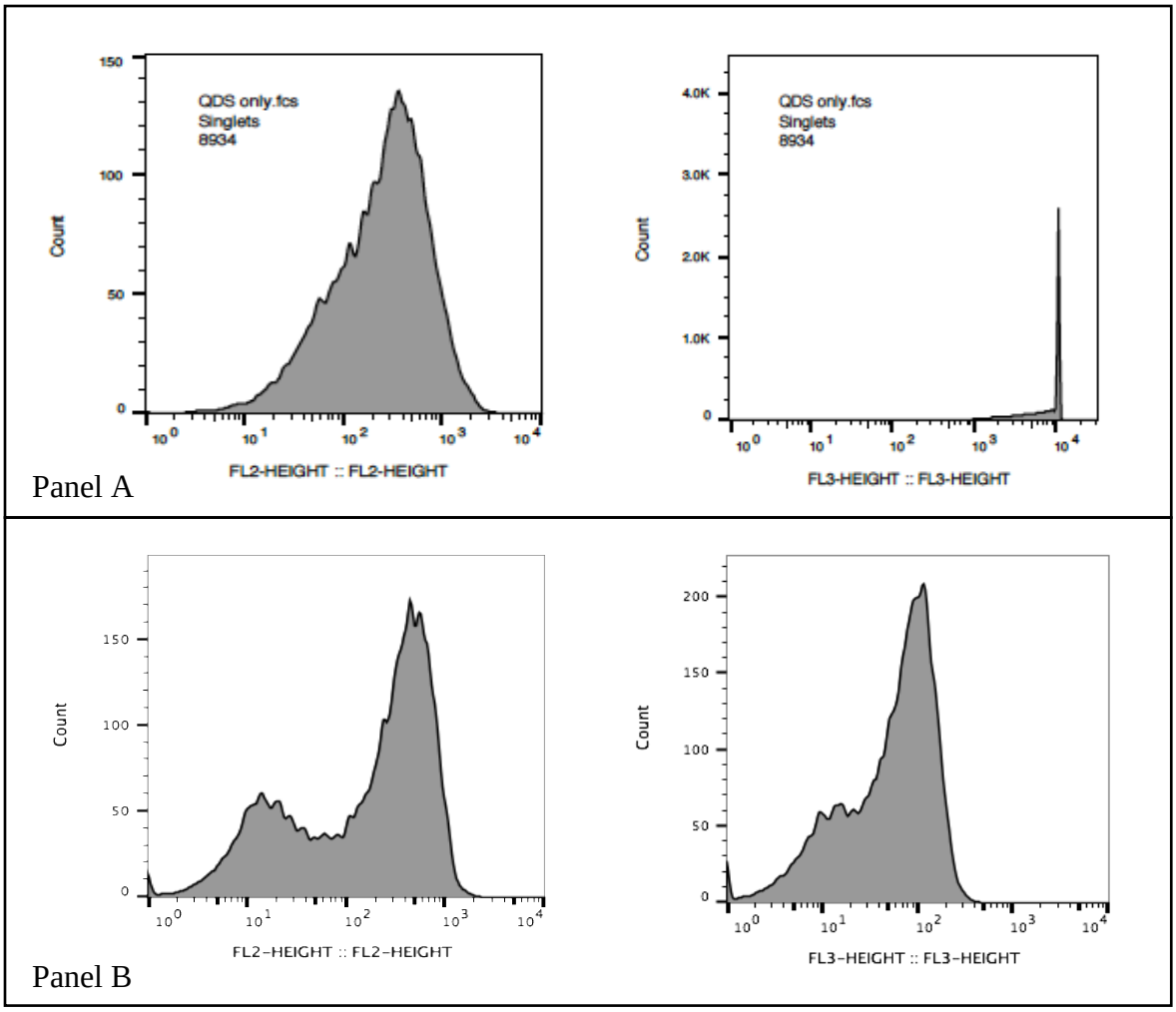

Figure 14: Median fluorescence intensity of Quantum dots (Panel A) and JC-10 (Panel B) in FL2 (left) and FL3 (Right). Hepa- V cells were treated with 20 nM QDs for 24 hours and analyzed using flow cytometry. The median fluorescence intensity of QDs in both FL2 (panel A, left) and FL3 (Panel A, right) is shown. The median fluorescence intensity of JC-10 treated cells in both FL2 (panel B, left) and FL3 (panel B, right) is shown.

The median fluorescence intensity of QDs in cells is similar to that of control cells with JC-10 stain only. Thus, the result showed that the background of QDs was not responsible for the data collected in FL2. Also, the result showed that QD fluoresces

remarkably higher when detected through FL3 more than 37-fold increment as compared to FL2.

CHAPTER IV

DISCUSSION

The TOPO-PMAT QDs used in this study are the group of QDs that would be used in imaging and medical purposes due to their extraordinary properties. These QDs are highly soluble and stable in aqueous environments.[8] The carboxylic functional group attached to the coating makes these QDs applicable for ligand attachment which would be very helpful in medical applications.

The cells used in this study are mouse liver cells (Hepa-V) and represent the cells of the organ which TOPO-PMAT may encounter if used for medical purposes. QDs with a bigger diameter than 5.5 nm are most likely deposited in the liver.[17] The diameter of TOPO-PMAT QDs used in this experiment is 12.7±0.5 nm[8], so these are most likely to be deposited in liver. Also as the size increases, the retention time of QDs in liver increases.[19] Since the liver is the target organ for the QDs of this size, the experiment performed in liver cells is representative of the effect that these QDs may have in liver when used *in vivo*.

The analysis of cells using flow cytometry after treating with QDs for 24 hours showed that the QDs were present inside the cells and that the majority of the QDs' fluorescence was detected through channel (FL3) (Figure 14, panel A). The finding was similar to previous work done in the Thomas research lab in Hepa-1c1c7 (CR-17) cells.[27] Hepa-1c1c7 cells are also mouse liver cells but with enhanced glutathione levels. The

result showed that Hepa-1c1c7 cells were able to uptake and internalize the QDs after 4 hours of treatment.[27] Smith et al. (2012) showed that, nearly all HepG2 (human liver cells) were able to internalize TOPO-PMAT QDs.[36] Similar studies with different cells (human macrophages, human kidney cells) confirmed that the QDs were internalized by these cells.[8] These data showed that TOPO-PMAT QDs can be readily internalized by cells when the QDs come in contact with live cells. Hence a thorough study should be undertaken before considering the use of these QDs *in vivo* as they can be readily internalized by many different types of cells.

Our results showed that the QDs did not have any significant effect on cell viability of Hepa-V cells. This result is similar to previous studies in human hepatocytes cells. Human hepatocytes did not show any decrease in cell viability when treated with 2 nM to 40 nM TOPO-PMAT QDs over 24-48-hour period.[36] Although our experiment did not show any significant decrease in cell viability, the treatment of cells with 2 nM, 20 nM and 40 nM QDs showed a trend of decreased cell viability by 21.5%, 20.9% and 13.8% respectively. The cell viability decreased by 20% in lower concentration of treatment while it decreased by only 13.8% at higher concentration treatment. The finding is similar to the McConnachie and colleagues' cell viability experiment conducted in human kidney cells in which the percent of cell viability increased as the concentration of TOPO-PMAT QDs increased to 40 nM.[8] This can be attributed to the activation of metabolic function of cells to make Nicotinamide adenine dinucleotide phosphate (NAD(P)H) more available under stress that may have been produced due to

exposure to QDs.[37] The presence of more NAD(P)H allows cells to remove more ROS using glutathione peroxidase for example, which converts hydrogen peroxide to water and oxygen.

Similarly, our results showed that there was not a significant change in ATP production when cells were treated with 2 nM, 20 nM and 40 nM of QDs. The ATP production showed a decreased trend, by only 2% when treated with 2 nM and 20 nM QDs, and by 14% when treated with 40 nM QDs. This trend showed that the amount of ATP produced by cells was constant and cells were able to maintain the amount of ATP produced. In previous studies it was shown that cells under stress are triggered to produce more ATP.[38] The level of intracellular ATP increases as a result of induced stress.[38] The release of ATP is a response of cells to induced stress. When cells were treated with different concentrations of QDs, cells were exposed to the stress. It is possible that in response to the QDs induced stress, cells started generating intracellular ATP. The intracellular ATP can be generated from glycolysis and other metabolism pathways such as the citric acid cycle in order to regulate the normal function of cells. When cells are treated with 40 nM of QDs, the ATP production trend decreased compared to control and other treatment cells. The stress from higher concentration treatment may have been more than the cells could handle as a result of which the ATP concentration decreased as compared to the other treatments.

The energy produced from oxidizing substrates in the electron transport chain is used in pumping protons across the inner membrane to the intermembrane space, which

results in a proton gradient and an electrochemical potential across the inner mitochondrial membrane known as the mitochondrial membrane potential. The proton motive force is used to generate ATP through ATP synthase. The measure of mitochondrial membrane potential is a sign of healthy and functioning cells. The result showed that the mitochondrial membrane potential decreased significantly when treated with 20 nM and 40 nM of QDs. Interestingly, mitochondrial membrane potential increases slightly when treated with 2 nM QDs. Similar studies on the effect of CdTe QDs on mitochondria showed that the mitochondria swell in the presence of QDs. They permeablize the mitochondrial inner membrane to H^+ and K^+ ions. These ions play an important role in distribution of charges across the inner mitochondrial membrane. The disturbance in this distribution of charges decreases the proton electrochemical gradient. This effect increased as the concentration of QDs increases from 50 nM to 50 μM.[39] The appropriate level of ion concentration is very important for the proper functioning of the mitochondria for the energy generation through the proton electrochemical potential gradient. In the presence of QDs the balance of these appropriate ion gradients is disturbed and the membrane potential decreases. The decrease in membrane potential indicates mitochondrial uncoupling. Uncoupling of mitochondria disrupts the process of ATP formation and ROS production.

A ROS assay was performed using CellRox green dye and the result showed that the production of ROS decreases when treated with different concentrations of QDs in two experiments. ROS are produced in cells as a by-product of ATP formation through

oxidative phosphorylation. Cells have their own antioxidant process to remove these ROS through reaction with superoxide dismutase and glutathione peroxidase. However, if cells start producing more ROS, the cells' natural antioxidant system may not be able to remove ROS giving rise to the presence of ROS in cells putting cells under oxidative stress. So the measurement of ROS when they are exposed to QDs is a way to determine the oxidative stress cells are going through.

The trend in both the experiments showed that ROS production decreased when treated with different concentration of QDs. Even though the flow cytometer was not functioning and cells had to be stored in the refrigerator for more than two hours before analysis, the trend of decreased ROS production in cells treated with QDs were similar in both experiments (Figure 13). Similar effects had been shown when cells are treated with uncoupling protein such as UCP 3 and UCP 1.[39] The presence of these proteins plays a role in uncoupling oxidative phosphorylation which reduces the mitochondrial membrane potential. We observed a significant decrease in mitochondrial membrane potential in cells treated with QDs. When mitochondria started depolarizing and the mitochondrial membrane potential decreased in the presence of uncoupling protein UCP 3 an UCP 1, the production of ROS was decreased which is in parallel to our findings. In addition, a study on the effect of MPA-CdSe/ZnS QDs on plant cells (*Sativa* cells) showed that cells responded to oxidative stress by increasing the antioxidant enzyme systems such as superoxide dismutase.[40] When cells are put under stress they respond to it by upregulating antioxidant enzymes.[41] It is possible that when cells were treated with QDs,

cells were under stress and upregulated the antioxidant enzyme as a result of which ROS production decreased.

However, other studies showed the increase in ROS in spite of an increase in antioxidant enzyme. The study was performed on liver cells of *Mus musculus* mouse (AML 12) treated with 20 µg/mL- 40 µg/mL CdTe QDs for 24 hours, which showed a significant increase in ROS.[42] The doses used in this experiment were very high compared to our experiment. It is possible that at lower doses (2 nM – 40 nM), the increased function of antioxidant systems is enough to remove the ROS and when the concentration of QDs treatment increases it is difficult for cells to remove ROS in spite of upregulation of antioxidant enzymes.

The QDs used in this study are composed of a CdSe/ZnS core/shell. Studies have shown that CdSe/ZnS QDs treated MCF-7 cells showed the presence of cadmium to be low to none when detected by Cd^{2+} cell assay compared to other QDs such as CdTe QDs. Also it was found that CdSe/ZnS QDs were non-toxic in terms of cell viability. In addition, the study showed that upon photoxidation CdTe QDs generate oxidative stress which was not found in ZnS coated QDs.[43] Since the CdSe core of the QDs used in our studies were covered with ZnS, it is possible that we observed mild toxicity due to this protective shell. The structure of QDs with ZnS may be manufactured in such a way that they remain intact for a long period of time and with less leaking of the core component cadmium which is associated with toxicity to cells.[24]

The internalization and toxic effects caused by QDs also depends upon the growth

medium used in cell culture. Several nanoparticles such as QDs are known to form coronas around them as the proteins in the growth media is absorbed by them. This may mitigate the effects of QDs in cells.[44] The type of protein coronas formed around QDs depends upon the protein components added to the media. Studies have shown that the use of fetal calf serum (FCS) in media may agglomerate the nanoparticles showing no or low toxicity in cells.[45] In our study all cells were grown in DMEM/F12 media supplemented with 10% Nu-serum which is substituted for the FCS in the medium and shows similar growth of cells. Nu-serum may have resulted in agglomeration of QDs used in this experiment which may have resulted in no significant effect in cell viability. However, a review paper on the formation of protein coronas states that the QDs with amphiphilic coatings do not form large protein coronas compared to hydrophilic QDs.[44] The QDs used in our study were amphiphilic QDs which may not have formed the coronas and were not involved in mitigating the toxic effect of QDs. Hence, the observed result may not be due to the formation of protein coronas around QDs. The QDs used may be less toxic due to the presence of ZnS shell, TOPO-PMAT coating and carboxylic acid functionalization. The shell and coating acted as a protective layer around the core of QDs and prevented leaking of cadmium from the core.

CHAPTER V

CONCLUSION

This study found that the TOPO-PMAT coated CdSe/ZnS QDs did not result in significant decrease in cell viability and ATP production. In addition, the result showed that these QDs resulted in a decrease in mitochondrial membrane potential which denotes uncoupled mitochondria. Although the data may not be reliable due to instrument malfunction, we observed a decrease in the production of reactive oxygen species (ROS). These results on Hepa-V cells suggest that similar effects may be seen on liver cells if used *in vivo* in humans.

These results showed that the use of TOPO- PMAT QDs is mildly toxic to cells indicated by a trend towards decreasing cell viability, ATP production and a significant decrease in mitochondrial membrane potential. At the lower concentration (2 nM), results showed minimal effect on cell viability, ATP production and mitochondrial membrane potential after a 24-hour treatment or exposure to QDs. This might indicate that it is safe to use QDs at lower concentrations for *in vivo* medical applications. However, caution should be applied if using in higher concentrations (20 nM or 40 nM) as the QDs may have some detrimental effects in organisms.

REFERENCES

(1) United States National Nanotechnology Initiative. Nanotechnology 101 http://www.nano.gov/nanotech-101 (accessed Apr 15, 2016).

(2) Jong, W.; Borm, P. Drug Delivery and Nanoparticles : Applications and Hazards. *Int. J. Nano Med.* **2008**, *3* (2), 133–149.

(3) Hauck, T. S.; Anderson, R. E.; Fischer, H. C.; Newbigging, S.; Chan, W. C. W. In vivo Quantum-Dot Toxicity Assessment. *Small* **2010**, *6* (1), 138–144.

(4) Kessler, R. Engineered nanoparticles in consumer products: understanding a new ingredient. *Env. Health Perspect* **2011**, *119* (3), A120–A125.

(5) Rosenthan, S.; Chang, J.; Kovtun, O.; McBride, J.; Tomlison, I. Biocompatible quantum dots for biological applications. *Chem. Biol.* **2011**, *18*, 10–24.

(6) Lovrić, J.; Cho, S. J.; Winnik, F. M.; Maysinger, D. Unmodified Cadmium Telluride Quantum Dots Induce Reactive Oxygen Species Formation Leading to Multiple Organelle Damage and Cell Death. *Chem. Biol.* **2005**, *12* (11), 1227–1234.

(7) Allen, P. M.; Bawendi, M. G. Ternary I−III−VI Quantum Dots Luminescent in the Red to Near-Infrared. *J. Am. Chem. Soc.* **2008**, *130* (29), 9240–9241.

(8) McConnachie, L. A.; White, C. C.; Botta, D.; Zadworny, M. E.; Cox, D. P.; Beyer, R. P.; Hu, X.; Eaton, D. L.; Gao, X.; Kavanagh, T. J. Heme oxygenase expression as a biomarker of exposure to amphiphilic polymer-coated CdSe/ZnS quantum dots. *Nanotoxicology* **2013**, *7* (2), 181–191.

(9) KAUL, Z.; Tomoko, T.; KAUL, S.; Takashi, H.; Renu, W.; Kazunari, T. Mortalin imaging in normal and cancer cells with quantum dot immuno-conjugates. *Cell Res.* **2003**, *13* (6), 503–507.

(10) Yang, L.; Mao, H.; Wang, Y. A.; Cao, Z.; Peng, X.; Wang, X.; Duan, H.; Ni, C.; Yuan, Q.; Adams, G.; et al. Single Chain Epidermal Growth Factor Receptor Antibody Conjugated Nanoparticles for in vivo Tumor Targeting and Imaging. *Small* **2008**, *5* (2), 235–243.

(11) Bagalkot, V.; Gao, X. siRNA-Aptamer Chimeras on Nanoparticles: Preserving Targeting Functionality for Effective Gene Silencing. *ACS Nano* **2011**, *5* (10), 8131–8139.

(12) Kim, J.; Park, Y.; Yoon, T. H.; Yoon, C. S.; Choi, K. Phototoxicity of CdSe/ZnSe quantum dots with surface coatings of 3-mercaptopropionic acid or tri-n-octylphosphine oxide/gum arabic in Daphnia magna under environmentally relevant UV-B light. *Aquat. Toxicol.* **2010**, *97* (2), 116–124.

(13) Derfus, A. M.; Chan, W. C. W.; Bhatia, S. N. Probing the Cytotoxicity of Semiconductor Quantum Dots. *Nano Lett.* **2004**, *4* (1), 11–18.

(14) Wiecinski, P. N.; Metz, K. M.; King Heiden, T. C.; Louis, K. M.; Mangham, A. N.; Hamers, R. J.; Heideman, W.; Peterson, R. E.; Pedersen, J. A. Toxicity of Oxidatively Degraded Quantum Dots to Developing Zebrafish (Danio rerio). *Environ. Sci. Technol.* **2013**, *47* (16), 9132–9139.

(15) Clift, M. J. D.; Brandenberger, C.; Rothen-Rutishauser, B.; Brown, D. M.; Stone, V. The uptake and intracellular fate of a series of different surface coated quantum dots in vitro. *Toxicology* **2011**, *286* (1-3), 58–68.

(16) Edmund, A. R.; Kambalapally, S.; Wilson, T. A.; Nicolosi, R. J. Encapsulation of cadmium selenide quantum dots using a self-assembling nanoemulsion (SANE) reduces their in vitro toxicity. *Toxicol. In Vitro* **2011**, *25* (1), 185–190.

(17) Soo Choi, H.; Liu, W.; Misra, P.; Tanaka, E.; Zimmer, J. P.; Itty Ipe, B.; Bawendi, M. G.; Frangioni, J. V. Renal clearance of quantum dots. *Nat. Biotechnol.* **2007**, *25* (10), 1165–1170.

(18) Su, Y.; Peng, F.; Jiang, Z.; Zhong, Y.; Lu, Y.; Jiang, X.; Huang, Q.; Fan, C.; Lee, S.-T.; He, Y. In vivo distribution, pharmacokinetics, and toxicity of aqueous synthesized cadmium-containing quantum dots. *Biomaterials* **2011**, *32* (25), 5855–5862.

(19) Daou, T. J.; Li, L.; Reiss, P.; Josserand, V.; Issabelle, T. Effect of Poly(ethylene glycol) Length on the in Vivo Behavior of Coated Quantum Dots. *Langmuir* **2009**, *25*, 3040–3044.

(20) Geys, J.; Nemmar, A.; Verbeken, E.; Smolders, E.; Ratoi, M.; Hoylaerts, M. F.; Nemery, B.; Hoet, P. H. Acute toxicity and prothrombotic effects of quantum dots: impact of surface charge. *Environ. Health Perspect.* **2008**, *116* (12), 1607.

(21) Clift, M. J. D.; Varet, J.; Hankin, S. M.; Brownlee, B.; Davidson, A. M.; Brandenberger, C.; Rothen-Rutishauser, B.; Brown, D. M.; Stone, V. Quantum dot cytotoxicity in vitro : An investigation into the cytotoxic effects of a series of

different surface chemistries and their core/shell materials. *Nanotoxicology* **2011**, *5* (4), 664–674.

(22) Mahendra, S.; Zhu, H.; Colvin, V. L.; Alvarez, P. J. Quantum dot weathering results in microbial toxicity. *Environ. Sci. Technol.* **2008**, *42* (24), 9424–9430.

(23) Fitzpatrick, J. A. J.; Andreko, S. K.; Ernst, L. A.; Waggoner, A. S.; Ballou, B.; Bruchez, M. P. Long-term Persistence and Spectral Blue Shifting of Quantum Dots in Vivo. *Nano Lett.* **2009**, *9* (7), 2736–2741.

(24) Chan, W.-H.; Shiao, N.-H.; Lu, P.-Z. CdSe quantum dots induce apoptosis in human neuroblastoma cells via mitochondrial-dependent pathways and inhibition of survival signals. *Toxicol. Lett.* **2006**, *167* (3), 191–200.

(25) Kowaltowski, A.; Souza-Pinto, nadja; Castilho, R.; Vercesi, A. Mitochondria and reactive oxygen species. *Free Radic. Biol. Med.* **2009**, *47*, 333–343.

(26) Animal mitochondrion diagram en (edit). http://en.wikipedia.org/ wiki/File:Animal mitochondrion_diagram_en (accessed Apr 25, 2016).

(27) Rosario, S. Do Quantum Dots Disrupt Mitochondrial Function in Murine Hepatocytes? M.S. Thesis, Central Washington University, Ellensburg, WA, June 2012.

(28) Ballou, B.; Lagerholm, B. C.; Ernst, L. A.; Bruchez, M. P.; Waggoner, A. S. Noninvasive Imaging of Quantum Dots in Mice. *Bioconjug. Chem.* **2004**, *15* (1), 79–86.

(29) Botta, D.; Franklin, C.; White, C.; Krejsa, C.; Dabrowski, M.; Pierce, R.; Fausto, N.; Kavanagh, T. Glutamate-cysteine ligase attenuates TNF-induced mitochondrial injury and apoptosis. *Free Radic. Biol. Med.* **2004**, *37* (5), 632–642.

(30) Ronner, P.; Friel, E.; Czerniawski, K.; Frankle, S. Luminometric assays of ATP, phosphocreatine and and creatine for estimation of free ADP and free AMP. *Anal. Biochem.* **1999**, *275*, 208–216.

(31) Abcam. JC-10 Mitochondrial Assay Kit http://www.abcam.com/jc-10-mitochondrial-membrane-potential-assay-kit-microplate-ab112134-references.html (accessed May 12, 2016).

(32) Kataoka, M.; Fukura, Y.; Shinohara, Y.; Baba, Y. Analysis of mitochondrial membrane potential in the cells by microchip flow cytometry. *Electrophoresis* **2005**, *26* (15), 3025–3031.

(33) Johnson, sam. Light Microscopy Core Facility http://microscopy.duke.edu/sampleprep/if.html (accessed Apr 15, 2016).

(34) CellROX Green Reagent, for oxidative stress detection - Thermo Fisher Scientific https://www.thermofisher.com/order/catalog/product/C10444 (accessed May 12, 2016).

(35) Xia Chen; Thibeault, S. Effect of DMSO concentration, cell density and needle gauge on the viability of cryopreserved cells in three dimensional hyaluronan hydrogel; IEEE, 2013; pp 6228–6231.

(36) Smith, W. E.; Brownell, J.; White, C. C.; Afsharinejad, Z.; Tsai, J.; Hu, X.; Polyak, S. J.; Gao, X.; Kavanagh, T. J.; Eaton, D. L. In Vitro Toxicity Assessment of Amphiphillic Polymer-Coated CdSe/ZnS Quantum Dots in Two Human Liver Cell Models. *ACS Nano* **2012**, *6* (11), 9475–9484.

(37) Naoi, T.; Shibuya, N.; Inoue, H.; Mita, S.; Kobayashi, S.; Watanabe, K.; Orino, K. The effect of tert-butylhydroquinone-induced oxidative stress in MDBK cells using XTT assay: implication of tert-butylhydroquinone-induced NADPH generating enzymes. *J. Vet. Med. Sci.* **2010**, *72* (3), 321–326.

(38) Ahmad, S.; Ahmad, A.; Ghosh, M.; Leslie, C. C.; White, C. W. Extracellular ATP-mediated Signaling for Survival in Hyperoxia-induced Oxidative Stress. *J. Biol. Chem.* **2004**, *279* (16), 16317–16325.

(39) Bezaire, V.; Seifert, E. L.; Harper, M.-E. Uncoupling protein-3: clues in an ongoing mitochondrial mystery. *FASEB J.* **2007**, *21* (2), 312–324.

(40) Santos, A. R.; Miguel, A. S.; Macovei, A.; Maycock, C.; Balestrazzi, A.; Oliva, A.; Fevereiro, P. CdSe/ZnS Quantum Dots trigger DNA repair and antioxidant enzyme systems in Medicago sativa cells in suspension culture. *BMC Biotechnol.* **2013**, *13* (1), 111.

(41) Halliwell, B. Reactive Species and Antioxidants. Redox Biology Is a Fundamental Theme of Aerobic Life. *PLANT Physiol.* **2006**, *141* (2), 312–322.

(42) Zhang, T.; Hu, Y.; Tang, M.; Kong, L.; Ying, J.; Wu, T.; Xue, Y.; Pu, Y. Liver Toxicity of Cadmium Telluride Quantum Dots (CdTe QDs) Due to Oxidative Stress in Vitro and in Vivo. *Int. J. Mol. Sci.* **2015**, *16* (10), 23279–23299.

(43) Cho, S. J.; Maysinger, D.; Jain, M.; Röder, B.; Hackbarth, S.; Winnik, F. M. Long-Term Exposure to CdTe Quantum Dots Causes Functional Impairments in Live Cells. *Langmuir* **2007**, *23* (4), 1974–1980.

(44) Foroozandeh, P.; Aziz, A. A. Merging Worlds of Nanomaterials and Biological Environment: Factors Governing Protein Corona Formation on Nanoparticles and Its Biological Consequences. *Nanoscale Res. Lett.* **2015**, *10* (1).

(45) Drescher, D.; Orts-Gil, G.; Laube, G.; Natte, K.; Veh, R. W.; Österle, W.; Kneipp, J. Toxicity of amorphous silica nanoparticles on eukaryotic cell model is determined by particle agglomeration and serum protein adsorption effects. *Anal. Bioanal. Chem.* **2011**, *400* (5), 1367–1373.

APPENDICES

APPENDIX A

Preliminary data using C_{60}

Cell Viability

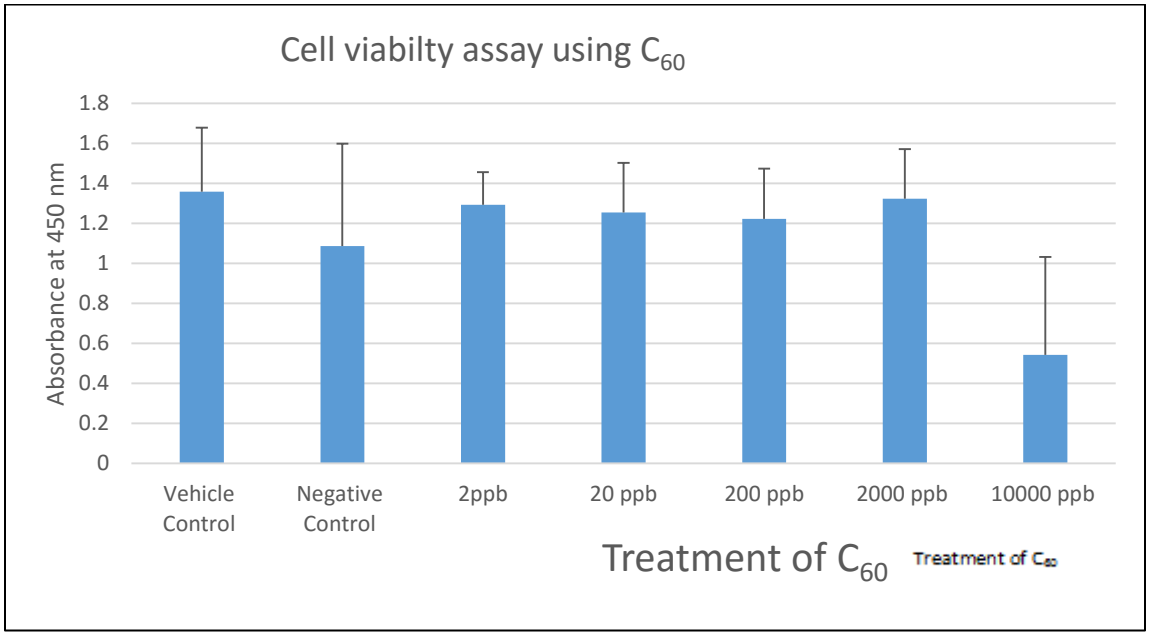

Figure A1. Cell viability after 24-hr exposure to C60**.** Liver cell mitochondrial dehydrogenase activity measured by the water soluble MTT assay (WST-8). Analysis by 1-Way ANOVA ($p<0.05$, $n=6$), indicates a significant effect of C_{60} on metabolic cell death. Negative control cells were treated with 20% DMSO for 1 hr.

ATP Assay

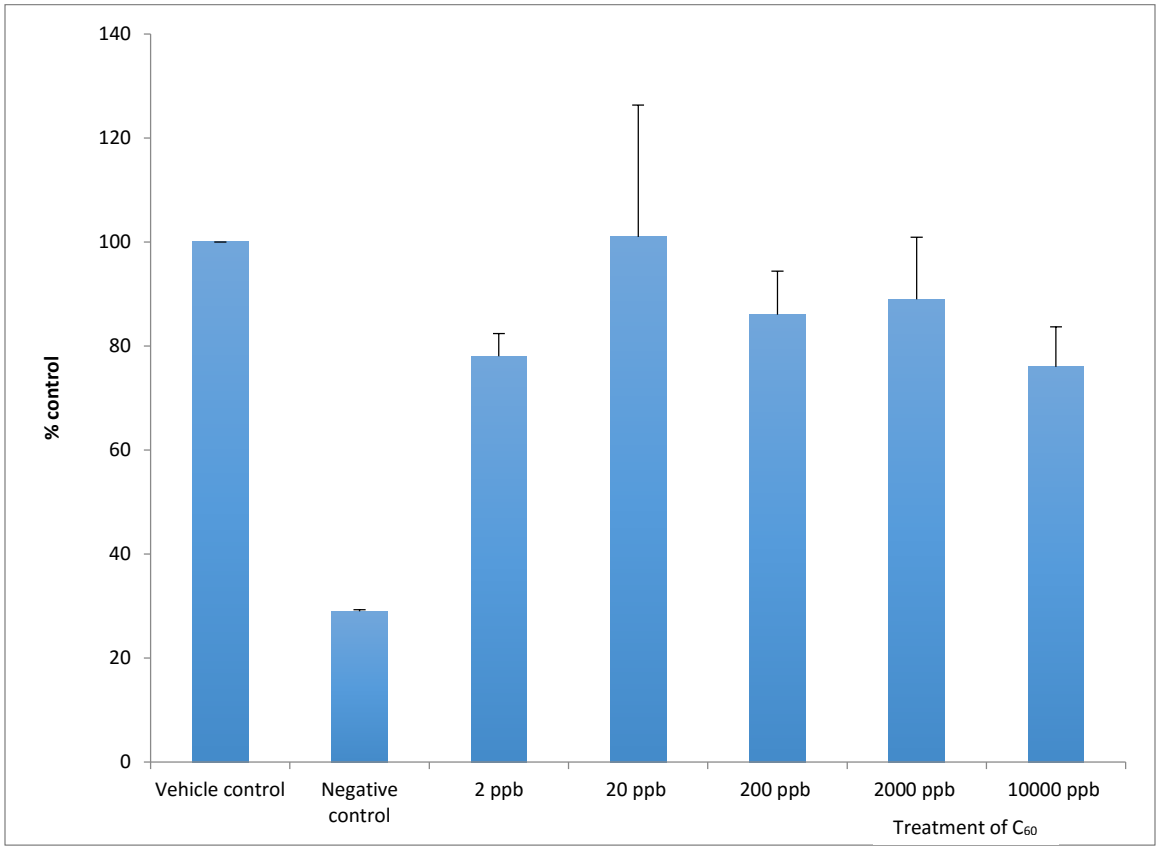

Figure A2: ATP production in liver cells after 24-hr exposure to C_{60}**.** ATP production of liver cells was determined by the Luciferase/luciferin luminescence assay. Vehicle control consists of DMEM and the 7.5% BSA in PBS. Negative control cells were treated with 10 μM Antimycin A for 6 hours. ($P > 0.05$, n=9). ATP values of the control cells ranged between 22 nM and 79 nM per 5000 cells.

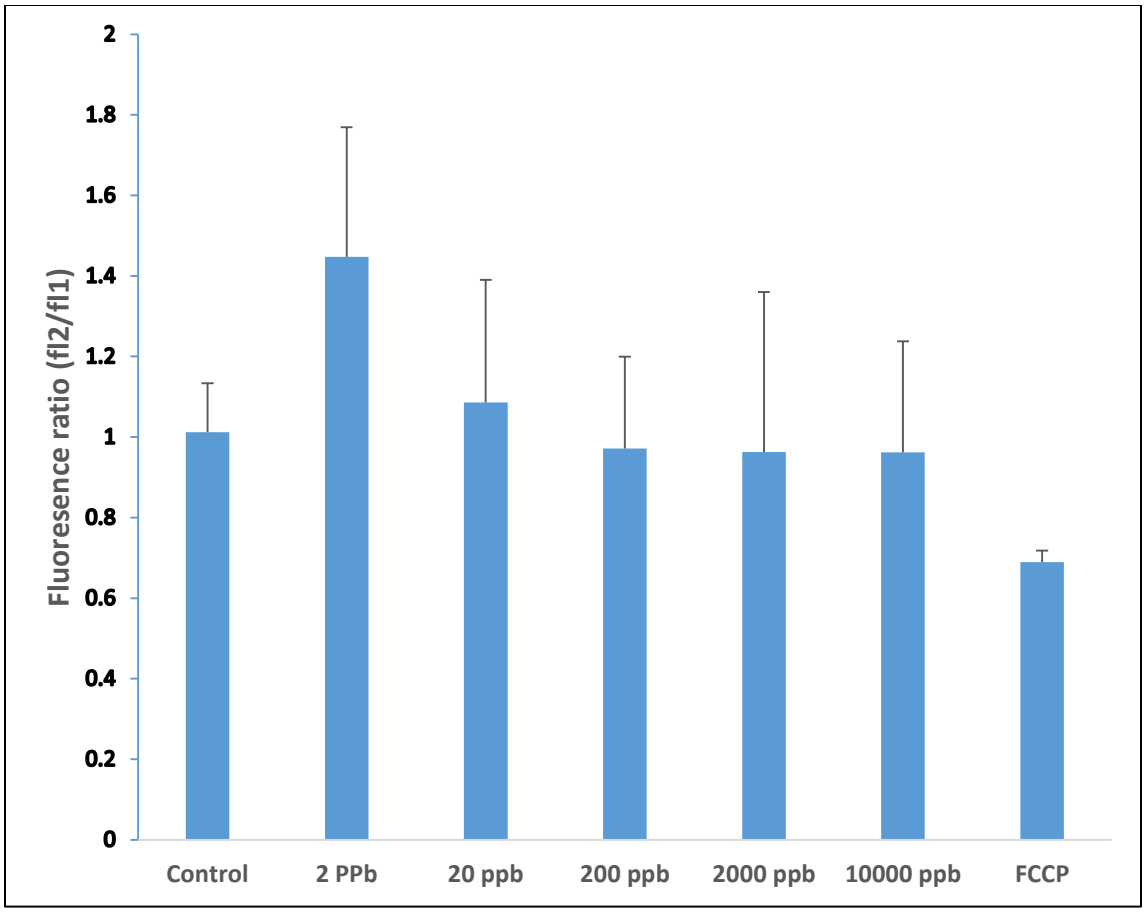

Figure A3. Mitochondrial membrane potential in liver cells after 24-hr exposure to C_{60}**.** JC-10 dye (20 µM) was added to Hepa-V liver cells and incubated for 30 min. Negative control cells were treated with FCCP (5 µM) and incubated for 10 min. The median fluorescence intensities for both J-aggregates and monomeric forms of JC-10 were measured at Ex/Em = 488/590 nm and 488/525 nm with flow cytometry and their ratio was calculated.

APPENDIX B

STATSTICAL ANALYSIS (QDs Study)

Cell Viability

ANOVA						
Source of Variation	*SS*	*df*	*MS*	*F*	*P-value*	*F crit*
Between Groups	0.015184438	3	0.005061479	2.594869305	0.082553804	3.127350005
Within Groups	0.037060867	19	0.001950572			
Total	0.052245304	22				

ATP Assay

ANOVA						
Source of Variation	*SS*	*df*	*MS*	*F*	*P-value*	*F crit*
Between Groups	541.1337196	3	180.3779065	1.846785609	0.174871735	3.15990759
Within Groups	1758.082964	18	97.67127576			
Total	2299.216683	21				

Mitochondrial Membrane Potential Assay

ANOVA						
Source of Variation	*SS*	*df*	*MS*	*F*	*P-value*	*F crit*
Between Groups	35.37440882	4	8.843602204	64.85889198	0.000169741	5.192167773
Within Groups	0.681757114	5	0.136351423			
Total	36.05616593	9				

APPENDIX C

FLOW CYTOMETRY DOT PLOTS and HISTOGRAMS FOR QDs

Mitochondrial Membrane Potential Assay

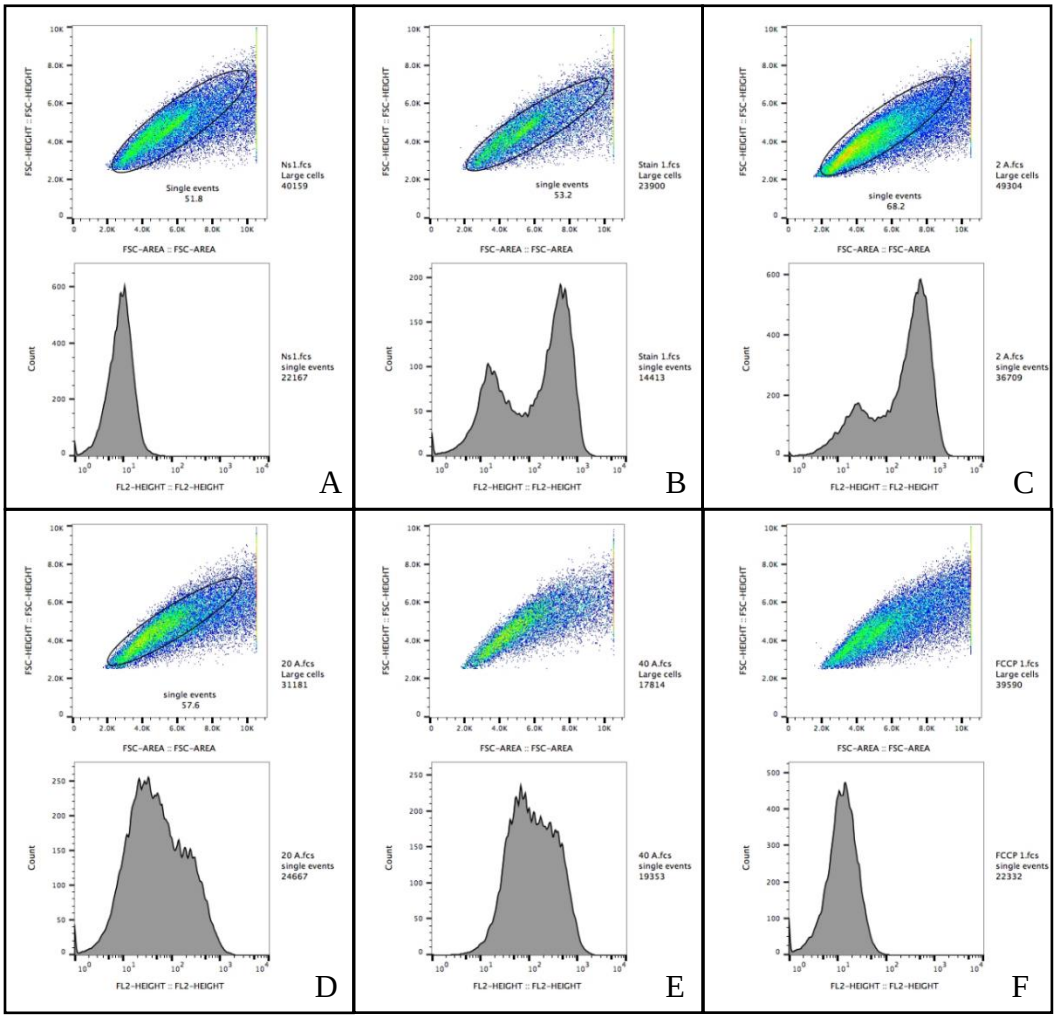

Figure A4: Flow cytometry dot plots and histogram showing gating and median fluorescence intensity at FL2 for mitochondrial membrane potential using JC-10 dye**.** A (Top, Bottom): Gating and FL2 intensity of no stain cells, B (Top, Bottom): Gating and FL2 intensity of stained cells, C (Top, Bottom): Gating and FL2 intensity of stained cells treated with 2 nM QDs, D (Top, Bottom): Gating and FL2 intensity of stained cells treated with 20 nM QDs, E(Top, Bottom):Gating and FL2 intensity of stained cells treated with 240 nM QDs, F(Top, Bottom):Gating and FL2 intensity of stained cells treated with 5 µM FCCP.

Reactive oxygen species

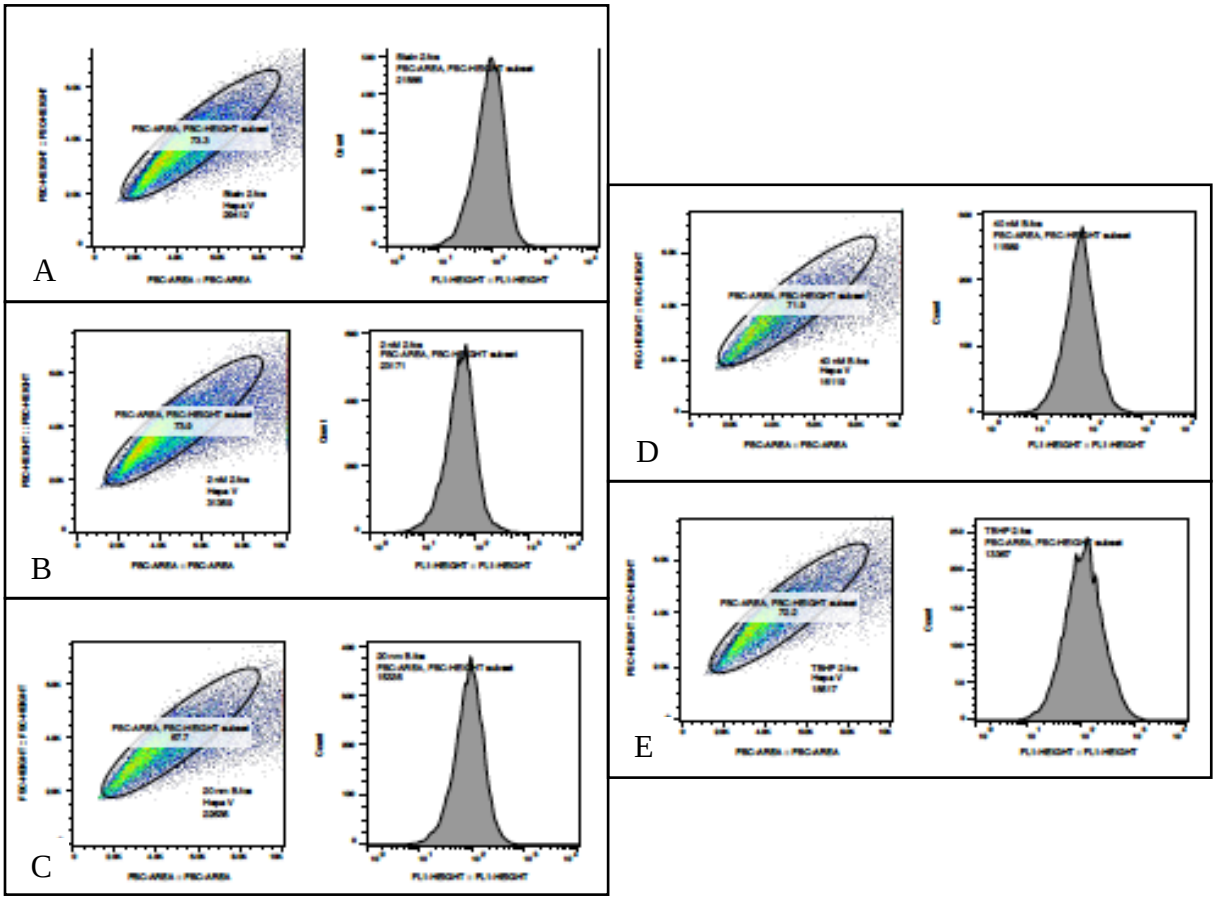

Figure A5: Flow cytometry dot plots and histogram showing gating and median fluorescence intensity at FL1 for reactive oxygen species (ROS) assay using CellRox green dye**.** A (Left, Right): Gating and FL1 median intensity of stained cells, B (Left, Right): Gating and FL1 intensity of 2 nM, C (Left, Right): Gating and FL1 intensity of stained cells treated with 20 nM QDs, D (Left, Right): Gating and FL1 intensity of stained cells treated with 40 nM QDs, E (Left, Right): Gating and FL1 intensity of stained cells treated with 10 µM of *tert*. butyl hydrogen peroxide.